Log-linear-complexity GLRT-optimal Noncoherent Sequence Detection for Orthogonal and RFID-oriented Modulations

Panos N. Alevizos, *Student Member, IEEE,* Yannis Fountzoulas, *Student Member, IEEE,*
George N. Karystinos, *Member, IEEE,* and Aggelos Bletsas, *Senior Member, IEEE*

***Abstract*—Orthogonal modulation, for example, frequency-shift keying (FSK) or pulse-position modulation (PPM), is primarily used in relatively-low-rate communication systems that operate in the power-limited regime. Optimal noncoherent detection of orthogonally modulated signals takes the form of sequence detection and has exponential (in the sequence length) complexity when implemented through an exhaustive search among all possible sequences. In this work, for the first time in the literature, we present an algorithm that performs generalized-likelihood-ratio-test (GLRT) optimal noncoherent sequence detection of orthogonally modulated signals in flat fading with log-linear (in the sequence length) complexity. Moreover, for Rayleigh fading channels, the proposed algorithm is equivalent to the maximum-likelihood (ML) noncoherent sequence detector. Simulation studies indicate that the optimal noncoherent FSK detector attains coherent-detection performance when the sequence length is on the order of 100, offering a 3–5dB gain over the typical energy (single-symbol) detector. While the conventional exhaustive-search approach becomes infeasible for such sequence lengths, the proposed implementation requires a log-linear only number of operations, opening new avenues for practical deployments. Finally, we show that our algorithm also solves efficiently the optimal noncoherent sequence detection problem in contemporary radio frequency identification (RFID) systems.**

***Index Terms*—Algorithm design and analysis, combinatorial mathematics, fading channels, FM0 coding, frequency-shift keying, generalized likelihood-ratio test, maximum-likelihood detection, noncoherent communication, pulse-position modulation, radio-frequency identification, sequence detection, wireless communication.**

I. Introduction

Orthogonal modulation is preferred to linear modulation (e.g., phase-shift keying (PSK), pulse-amplitude-modulation (PAM), quadrature amplitude modulation (QAM)) in relatively-low-rate communication systems that operate in the power-limited regime. A typical example is FSK which is primarily used (or considered for future use) in underwater communications [1]–[7], acoustic short-range communications [8], [9], power-line communications [10], [11], backscatter sensor networks and RFID [12]–[16], low-power wireless sensor networks [17], and cooperative communications [18]–[23]. To avoid the need for channel estimation (that induces added complexity at the receiver end and rate loss due to the necessary use of a pilot sequence), systems that utilize orthogonal modulation usually operate in the noncoherent mode; the receiver performs noncoherent (or blind) detection without any channel knowledge [8], [10], [13], [18]–[21], [23]–[27]. This is partly due to the simplicity of the single-symbol noncoherent detector which, for orthogonal modulation (e.g., FSK or PPM), is a simple energy detector [8], [18]–[21], [25]–[28].

However, due to channel-induced memory, the optimal noncoherent detector is no longer a single-symbol one but requires processing of the entire received sequence to make a decision on the entire data sequence, i.e., it is a sequence detector. In fact, noncoherent sequence detection may offer significant performance gains in comparison with conventional single-symbol noncoherent detection [29], [30]. This observation was first made in [31]–[34], in the context of M-ary PSK (MPSK), where it was shown that ML noncoherent sequence detection minimizes the sequence error probability, offering significant error rate performance gains over the conventional symbol-by-symbol noncoherent detection and attaining nearly-coherent detection performance for sufficiently long sequences. This is partly due to the fact that sequence detection exploits the correlation of the received symbols in the entire sequence (due to channel-induced memory), whereas symbol-by-symbol detection does not.

Regarding FSK modulation, noncoherent sequence detection has been considered in [10], [14], [23], [24], [35], [36]. Nevertheless, optimal sequence detection comes at a high price when implemented through an exhaustive search among all possible transmitted data sequences; its complexity is exponential in the sequence length [23], [35], [36]. In the context of power-line communications, to reduce the overall complexity, the authors in [10] propose a low-complexity suboptimal noncoherent FSK sequence detector. Work in [14], [16], in the context of scatter radio sensor networks, offered soft-decision metrics for noncoherent binary FSK sequence detection; however, each possible sequence belonged to a specific short block-length error-correcting (channel) code.

In this work, for the first time in the literature, we present an algorithm that performs GLRT-optimal noncoherent sequence detection of orthogonally modulated signals in flat fading

The authors are with the School of Electronic and Computer Engineering, Technical University of Crete, Chania, 73100 Greece (e-mail: {palevizos, ifountzoulas}@isc.tuc.gr, {karystinos, aggelos}@telecom.tuc.gr).

This work was supported by the ERC-04-BLASE project, executed in the context of the “Education & Lifelong Learning” Operational Program of the National Strategic Reference Framework (NSRF), General Secretariat for Research & Technology (GSRT), funded through European Union-European Social Fund and Greek national funds. This paper was presented in part at the IEEE International Conference on Acoustics, Speech, and Signal Processing (ICASSP 2015), Brisbane, Australia, April 2015.

with log-linear (in the sequence length) complexity. GLRT is independent of the fading channel distribution and, hence, is a practical option when the channel statistics are not known at the receiver. Moreover, we show that, for Rayleigh fading channels, the proposed algorithm is equivalent to the ML noncoherent sequence detector. Our algorithm utilizes principles that have been used for polynomial-complexity optimization in [37]–[40] and complements efficient optimal noncoherent detection techniques that have been developed for PSK [37], [38],[1] [42] and PAM or QAM [40], [43]–[45] signals.[2] We show that, as the sequence length increases, the proposed noncoherent scheme for orthogonally modulated signals attains nearly coherent performance, offering a 3–5dB gain over the typical energy (single-symbol) detector [8], [18]–[21], [25]–[28], whereas it does not require any channel knowledge. In contrast to the conventional exhaustive-search approach that requires an exponential number of operations, the proposed implementation of optimal[3] noncoherent detection requires a log-linear only (in the sequence length) number of operations, opening new avenues for practical deployments.

Moreover, we consider noncoherent sequence detection of FM0 signals. We recall that FM0 is a line-coding technique that is utilized by the current RFID standards [46]–[64]. For FM0, the optimal coherent detector operates on two consecutive received samples to make a decision for a single bit [46]. However, for noncoherent detection over channels whose coherence time spans more than two information symbols, such two-sample correlation is inadequate to allow optimal detection. In this work, we show that noncoherent sequence detection of zero-offset FM0 is equivalent to noncoherent sequence detection of uncoded binary FSK (BFSK). Hence, the proposed algorithm for orthogonally modulated signals also solves efficiently the optimal noncoherent detection problem in contemporary RFID systems. Finally, we show that noncoherent sequence detection of antipodal FM0 signals is equivalent to noncoherent sequence detection of uncoded binary PSK, allowing the use of relevant log-linear-complexity optimal sequence detectors [37], [38], [41], [42].

The rest of this paper is organized as follows. Section II presents the signal model for orthogonal modulation and the corresponding ML and GLRT noncoherent sequence detection algorithms. Sections III and IV describe how the new algorithms of Section II can be utilized for optimal noncoherent detection in contemporary RFID systems. In Section V, we study the performance of the proposed schemes. Finally, a few conclusions are drawn in Section VI.

Notation: Nonbold lower-case letters (e.g., x) will stand for variables. Vectors and matrices will be denoted by lower-case (e.g., $\mathbf{x}$) and capital (e.g., $\mathbf{A}$), respectively, bold characters. Symbols $(\cdot)^T$ and $(\cdot)^H$ will denote the transpose and hermitian, respectively, of a vector or matrix. Real-part operation is denoted by $\Re\{\cdot\}$. The proper complex Gaussian distribution with mean $\boldsymbol{\mu}$ and covariance matrix $\boldsymbol{\Sigma}$ is denoted by $\mathcal{CN}(\boldsymbol{\mu}, \boldsymbol{\Sigma})$. Finally, $\|\mathbf{x}\|$ stands for the euclidean norm of vector $\mathbf{x}$.

[1] The algorithm of [37], [38] reappeared in [41].

[2] The method in [40] applies to QAM constellations with independent in-phase and quadrature components.

[3] Throughout the paper, when we use the term "optimal sequence detection," we refer to GLRT-optimal sequence detection.

II. Orthogonal Modulation

In this section, we present a novel algorithm that performs optimal noncoherent sequence detection of orthogonally modulated signals in flat fading with log-linear complexity. We note that we consider a block flat-fading channel and our proposed algorithm performs GLRT-optimal detection under a Gaussian assumption about the noise. Moreover, under an added Rayleigh assumption about the channel, our algorithm is also the ML detector.

Although our developments hold for any orthogonally modulated signaling technique, we choose to present them in the context of FSK.

A. *Signal Model and Optimal Noncoherent Detection*

M-ary FSK (MFSK) utilizes M sub-carrier frequencies to modulate the information symbol $x \in \mathcal{M} \triangleq \{1, 2, \ldots, M\}$. For a single-symbol period, the transmitted MFSK waveform is given by $u_x(t)$ which is selected from the available set of M waveforms defined by [28]

$$u_m(t) = \sqrt{\frac{P}{T}} \mathsf{e}^{j2\pi f_m t}, \quad 0 \le t < T, \quad m = 1, 2, \ldots, M. \tag{1}$$

In (1), P and T denote signal strength and nominal duration, respectively, and $f_m, m = 1, 2, \ldots, M$, are the utilized frequencies which, in noncoherent FSK, must satisfy the orthogonality condition, i.e., $|f_m - f_{m'}| = k\frac{1}{T}$, for some $k \in \mathbb{N}$, $\forall m, m' \in \mathcal{M}$ with $m \neq m'$. If the modulated waveform is transmitted through a flat-fading channel [10], [23], [26], [35], [36], [65]–[67], then the received signal, after downconversion, is written as

$$r(t) = h u_x(t) + n(t) \tag{2}$$

where h is a complex number that models signal attenuation and phase change due to the channel[4] and $n(t)$ is a zero-mean complex Gaussian process with variance σ_w^2, modeling thermal noise at the receiver. The optimal receiver correlates the received signal $r(t)$ with all M signaling waveforms $u_1(t), u_2(t), \ldots, u_M(t)$ to produce samples

$$r_m = \frac{1}{\sqrt{P}} \int_0^T r(t) u_m^*(t) \mathsf{d}t, \quad m = 1, 2, \ldots, M. \tag{3}$$

If the orthogonality condition is satisfied, then

$$r_m = \begin{cases} \sqrt{P} h + n_m, & m = x, \\ n_m, & m \neq x, \end{cases} \tag{4}$$

where $n_1, n_2, \ldots, n_M$ are independent zero-mean circularly symmetric complex Gaussian variables with variance σ_w^2 [28].

[4] We assume that the channel fading coefficient is the same over each sub-carrier frequency.

Consequently, for a single-symbol duration, the received vector becomes

$$\underbrace{\begin{bmatrix} r_1 \\ r_2 \\ \vdots \\ r_M \end{bmatrix}}_{\mathbf{r}} = \sqrt{P}h\mathbf{e}_x + \underbrace{\begin{bmatrix} n_1 \\ n_2 \\ \vdots \\ n_M \end{bmatrix}}_{\mathbf{n}} \tag{5}$$

where $\mathbf{n} \sim \mathcal{CN}(\mathbf{0}, \sigma_w^2 \mathbf{I}_M)$ and

$$\mathbf{e}_x = [\underbrace{0 \ \ldots \ 0}_{x-1} \ \ 1 \ \ \underbrace{0 \ \ldots \ 0}_{M-x}]^T \tag{6}$$

is the xth column, $x = 1, 2, \ldots, M$, of the $M \times M$ identity matrix $\mathbf{I}_M$. For notation simplicity, we also define the set

$$\mathcal{I}_M \triangleq \{\mathbf{e}_1, \mathbf{e}_2, \ldots, \mathbf{e}_M\} \tag{7}$$

that consists of the M columns of $\mathbf{I}_M$.

If the actual channel realization is not available to the receiver and is modeled as a random variable, then this variable appears in consecutive received vectors implying that consecutive received vectors are no longer independent (even under the condition of known transmitted symbols). In other words, the channel induces memory in the received signal; as a result, optimal detection requires processing of a sequence of received vectors.

Let $\mathbf{x} = [x_1 \ x_2 \ \ldots \ x_N]^T \in \mathcal{M}^N$ be the transmitted $N \times 1$ information-symbol sequence. If $\mathbf{y}_1, \mathbf{y}_2, \ldots, \mathbf{y}_N$ are the corresponding received vectors (per information symbol) given by (5), then we may form the received vector for the entire sequence $\mathbf{x}$ as

$$\mathbf{y} \triangleq \begin{bmatrix} \mathbf{y}_1 \\ \mathbf{y}_2 \\ \vdots \\ \mathbf{y}_N \end{bmatrix} = \sqrt{P}h \underbrace{\begin{bmatrix} \mathbf{e}_{x_1} \\ \mathbf{e}_{x_2} \\ \vdots \\ \mathbf{e}_{x_N} \end{bmatrix}}_{\mathbf{s}} + \mathbf{w} \tag{8}$$

where $\mathbf{w} \sim \mathcal{CN}(\mathbf{0}, \sigma_w^2 \mathbf{I}_{MN})$, $\mathbf{s}$ is the column-wise concatenation of the N transmitted signal vectors $\mathbf{e}_{x_1}, \mathbf{e}_{x_2}, \ldots, \mathbf{e}_{x_N}$, and $\mathbf{y}$ is the column-wise concatenation of the N received signal vectors $\mathbf{y}_1, \mathbf{y}_2, \ldots, \mathbf{y}_N$. Both $\mathbf{s}$ and $\mathbf{y}$ have size $MN \times 1$.

The ML noncoherent detector maximizes the conditional probability density function (pdf) of $\mathbf{y}$ given $\mathbf{s}$, that is, the optimal decision is given by

$$\hat{\mathbf{s}}^{\mathrm{ML}} = \underset{\mathbf{s} \in \mathcal{I}_M^N}{\arg\max} \, f(\mathbf{y}|\mathbf{s}) \tag{9}$$

where $f(\cdot|\cdot)$ stands for the conditional pdf of the observation vector given the transmitted symbol sequence and

$$\mathcal{I}_M^N = \left\{ \begin{bmatrix} \mathbf{e}_{x_1} \\ \mathbf{e}_{x_2} \\ \vdots \\ \mathbf{e}_{x_N} \end{bmatrix} : \ \mathbf{e}_{x_i} \in \mathcal{I}_M, \ x_i \in \mathcal{M}, \ i = 1, 2, \ldots, N \right\}. \tag{10}$$

Note that $\|\mathbf{s}\|^2 = N$, for any $\mathbf{s} \in \mathcal{I}_M^N$. It can be shown that, for Rayleigh fading (i.e., $h \sim \mathcal{CN}(0, \sigma_h^2)$) [26], [47], [52], [58], [65], [67], the received symbol vector $\mathbf{y}$ given the transmitted sequence $\mathbf{s}$ follows a proper complex Gaussian distribution with mean $\mathbb{E}[\mathbf{y}|\mathbf{s}] = \mathbf{0}$ and covariance matrix

$$\mathbf{C}_{\mathbf{y}|\mathbf{s}} \triangleq \mathbb{E}\left[\mathbf{y}\mathbf{y}^H|\mathbf{s}\right] = P\sigma_h^2 \mathbf{s}\mathbf{s}^T + \sigma_w^2 \mathbf{I}_{MN}. \tag{11}$$

Consequently, the ML optimization problem in (9) can be rewritten as

$$\hat{\mathbf{s}}^{\mathrm{ML}} = \underset{\mathbf{s} \in \mathcal{I}_M^N}{\arg\max} \frac{1}{\left|\mathbf{C}_{\mathbf{y}|\mathbf{s}}\right|} \mathrm{e}^{-\mathbf{y}^H \mathbf{C}_{\mathbf{y}|\mathbf{s}}^{-1} \mathbf{y}}. \tag{12}$$

Exploiting identities for the determinant and inverse of a rank-1 update [68] and the fact that $\|\mathbf{s}\|^2 = N$, we obtain

$$\begin{aligned} \left|\mathbf{C}_{\mathbf{y}|\mathbf{s}}\right| &= \left|\sigma_w^2 \mathbf{I}_{MN} + P\sigma_h^2 \mathbf{s}\mathbf{s}^T\right| = \left|\sigma_w^2 \mathbf{I}_{MN}\right| \left(1 + \frac{P\sigma_h^2}{\sigma_w^2}\|\mathbf{s}\|^2\right) \\ &= \sigma_w^{2MN-2}\left(\sigma_w^2 + P\sigma_h^2\|\mathbf{s}\|^2\right) \\ &= \sigma_w^{2MN-2}\left(\sigma_w^2 + P\sigma_h^2 N\right) \end{aligned} \tag{13}$$

and

$$\begin{aligned} \mathbf{C}_{\mathbf{y}|\mathbf{s}}^{-1} &= \left(\sigma_w^2 \mathbf{I}_{MN} + P\sigma_h^2 \mathbf{s}\mathbf{s}^T\right)^{-1} \\ &= \frac{1}{\sigma_w^2}\mathbf{I}_{MN} - \frac{P\sigma_h^2}{\sigma_w^4 + P\sigma_h^2\sigma_w^2\|\mathbf{s}\|^2}\mathbf{s}\mathbf{s}^T \\ &= \frac{1}{\sigma_w^2}\mathbf{I}_{MN} - \frac{P\sigma_h^2}{\sigma_w^4 + P\sigma_h^2\sigma_w^2 N}\mathbf{s}\mathbf{s}^T. \end{aligned} \tag{14}$$

If we substitute (13) and (14) in (12), we obtain

$$\begin{aligned} \hat{\mathbf{s}}^{\mathrm{ML}} &= \underset{\mathbf{s} \in \mathcal{I}_M^N}{\arg\max} \Bigg\{ -\mathbf{y}^H \left(\frac{1}{\sigma_n^2}\mathbf{I}_{MN} - \frac{P\sigma_h^2}{\sigma_w^4 + P\sigma_h^2\sigma_w^2 N}\mathbf{s}\mathbf{s}^T\right)\mathbf{y} \\ &\quad - \ln\left(\sigma_w^{2MN-2}\left(\sigma_w^2 + P\sigma_h^2 N\right)\right) \Bigg\} \\ &= \underset{\mathbf{s} \in \mathcal{I}_M^N}{\arg\max} \left|\mathbf{s}^T \mathbf{y}\right|. \end{aligned} \tag{15}$$

Substituting $\mathbf{s} = [\mathbf{e}_{x_1}^T \ \mathbf{e}_{x_2}^T \ \ldots \ \mathbf{e}_{x_N}^T]^T$ in (15), the ML rule is rewritten in terms of the information sequence $\mathbf{x}$ as[5]

$$\hat{\mathbf{x}}^{\mathrm{ML}} = \underset{\mathbf{x} \in \mathcal{M}^N}{\arg\max} \left|y_1[x_1] + y_2[x_2] + \ldots + y_N[x_N]\right|. \tag{16}$$

The equivalent expressions (15) and (16) represent the optimal decision rule when the channel coefficient follows a Rayleigh distribution.

If, on the other hand, the channel distribution is not Rayleigh or is unknown, then we may consider joint channel estimation and data detection, i.e., GLRT sequence detection [44], according to which,

$$\begin{aligned} \hat{\mathbf{s}}^{\mathrm{GLRT}} &= \underset{\mathbf{s} \in \mathcal{I}_M^N}{\arg\min} \left\{ \min_{h \in \mathbb{C}} \left\|\mathbf{y} - \sqrt{P}h\mathbf{s}\right\|^2 \right\} \\ &= \underset{\mathbf{s} \in \mathcal{I}_M^N}{\arg\min} \left\|\mathbf{y} - \frac{\mathbf{s}^T\mathbf{y}}{\|\mathbf{s}\|^2}\mathbf{s}\right\|^2 \\ &= \underset{\mathbf{s} \in \mathcal{I}_M^N}{\arg\max} \frac{\left|\mathbf{y}^H\mathbf{s}\right|^2}{\|\mathbf{s}\|^2} = \underset{\mathbf{s} \in \mathcal{I}_M^N}{\arg\max} \left|\mathbf{s}^T\mathbf{y}\right|. \end{aligned} \tag{17}$$

[5] We use the notation $\mathbf{y}_n = \begin{bmatrix} y_n[1] \\ y_n[2] \\ \vdots \\ y_n[M] \end{bmatrix}$ to represent the $M \times 1$ vector $\mathbf{y}_n$, $n = 1, 2, \ldots, N$.

Hence, the ML optimization problem in (15) and the GLRT optimization problem in (17) are equivalent. This equivalence between noncoherent ML and GLRT has been also demonstrated in the context of equal-energy signals and uniformly distributed over $[0, 2\pi)$ channel phase [29], [43]. A straightforward approach to solve (15) and (17) (or, equivalently, (16)) would be an exhaustive search among all M^N sequences $\mathbf{x} \in \mathcal{M}^N$. However, such a solver would be impractical even for moderate values of N, since its complexity is on the order of $\mathcal{O}\big(M^N\big)$, i.e., it grows exponentially with N. In the following, we present an algorithm that solves the above problems with log-linear complexity $\mathcal{O}(N\log N)$. Similar algorithms have been developed for polynomial-time optimal noncoherent detection of PSK signals in [37], [38], [41], [42] and PAM or QAM signals in [40], [43]–[45].

B. Log-linear-complexity Optimal Detection

First, we present the proposed algorithm for BFSK ($M = 2$). Then, we generalize to any $M \geq 2$. In either case, we begin by rewriting the optimal detection rule in (16) as

$$\begin{aligned}
&\max_{\mathbf{x}\in\mathcal{M}^N} \left|y_1[x_1] + y_2[x_2] + \ldots + y_N[x_N]\right| \\
&= \max_{\mathbf{x}\in\mathcal{M}^N} \max_{\phi\in[0,2\pi)} \Re\left\{\mathsf{e}^{-j\phi}\left(y_1[x_1] + y_2[x_2] + \ldots + y_N[x_N]\right)\right\} \\
&= \max_{\phi\in[0,2\pi)} \max_{\mathbf{x}\in\mathcal{M}^N} \Big\{\Re\left\{\mathsf{e}^{-j\phi}y_1[x_1]\right\} + \Re\left\{\mathsf{e}^{-j\phi}y_2[x_2]\right\} + \ldots \\
&\qquad \ldots + \Re\left\{\mathsf{e}^{-j\phi}y_N[x_N]\right\}\Big\}. \qquad (18)
\end{aligned}$$

1) Optimal algorithm for $M = 2$: For a given point $\phi \in [0, 2\pi)$, the innermost maximization in (18) is separable for each x_n and, hence, splits into independent maximizations for any $n = 1, 2, \ldots, N$, as

$$\begin{aligned}
\hat{x}_n &= \underset{x_n\in\{1,2\}}{\arg\max} \Re\left\{\mathsf{e}^{-j\phi}y_n[x_n]\right\} \\
&\Leftrightarrow \Re\left\{\mathsf{e}^{-j\phi}y_n[1]\right\} \underset{\hat{x}_n=2}{\overset{\hat{x}_n=1}{\gtrless}} \Re\left\{\mathsf{e}^{-j\phi}y_n[2]\right\} \\
&\Leftrightarrow \Re\left\{\mathsf{e}^{-j\phi}(y_n[1] - y_n[2])\right\} \underset{\hat{x}_n=2}{\overset{\hat{x}_n=1}{\gtrless}} 0 \\
&\Leftrightarrow \cos\big(\phi - \angle y_n[1] - y_n[2]\big) \underset{\hat{x}_n=2}{\overset{\hat{x}_n=1}{\gtrless}} 0 \qquad (19)
\end{aligned}$$

where $\hat{x}_n$ is the decision on the nth information symbol x_n of the sequence of N consecutive symbols and $\angle z$ denotes the angle of the complex number z.

According to (18), to obtain the optimal sequence $\hat{\mathbf{x}}^{\mathrm{ML}}$ in (16), it suffices to let ϕ vary from 0 to 2π and, for each value of ϕ, determine the corresponding sequence $\hat{\mathbf{x}} = [\hat{x}_1\ \hat{x}_2\ \ldots\ \hat{x}_N]^T$ using (19) for $n = 1, 2, \ldots, N$. Then, one of the collected sequences that we meet as ϕ varies from 0 to 2π will be $\hat{\mathbf{x}}^{\mathrm{ML}}$.

Interestingly, as ϕ scans $[0, 2\pi)$, the decision $\hat{x}_n$ changes, according to (19), only when

$$\begin{aligned}
&\cos\big(\phi - \angle y_n[1] - y_n[2]\big) = 0 \\
&\Leftrightarrow \phi = \underbrace{\pm\frac{\pi}{2} + \angle y_n[1] - y_n[2] \pmod{2\pi}}_{\phi_n^{(1)},\,\phi_n^{(2)}}. \qquad (20)
\end{aligned}$$

Hence, the sequence decision $\hat{\mathbf{x}} = [\hat{x}_1\ \hat{x}_2\ \ldots\ \hat{x}_N]^T$ changes only at $\phi_1^{(1)}, \phi_1^{(2)}, \phi_2^{(1)}, \phi_2^{(2)}, \ldots, \phi_N^{(1)}, \phi_N^{(2)}$. In the following, we assume that the above $2N$ points are distinct and nonzero, i.e., $\phi_n^{(j)} \neq \phi_l^{(k)}$ and $\phi_n^{(j)} \neq 0$, for any $j, k \in \{1, 2\}$ and $n, l \in \{1, 2, \ldots, N\}$ with $n \neq l$. The case where the above assumption does not hold is examined separately in Footnote 6.

Since the $2N$ points are distinct, only one element of the sequence changes at each such point. If we sort the above points in ascending order, i.e.,

$$(\theta_1, \theta_2, \ldots, \theta_{2N}) = \mathsf{sort}\left(\phi_1^{(1)}, \phi_1^{(2)}, \phi_2^{(1)}, \phi_2^{(2)}, \ldots, \phi_N^{(1)}, \phi_N^{(2)}\right), \qquad (21)$$

then the decision $\hat{\mathbf{x}}$ remains constant in each one of the $2N$ intervals

$$C_0 = (0, \theta_1)\,,\ C_1 = (\theta_1, \theta_2)\,,\ \ldots,\ C_{2N-1} = (\theta_{2N-1}, \theta_{2N})\,. \qquad (22)$$

Note that we ignore $(\theta_{2N}, 2\pi)$ because it gives the same sequence $\hat{\mathbf{x}}$ with $C_0 = (0, \theta_1)$.

Our objective is the identification of the $2N$ sequences $\hat{\mathbf{x}}_0, \hat{\mathbf{x}}_1, \ldots, \hat{\mathbf{x}}_{2N-1}$ (that correspond to the $2N$ intervals $C_0, C_1, \ldots, C_{2N-1}$), one of which is $\hat{\mathbf{x}}^{\mathrm{ML}}$. We begin by setting $\phi = 0$ and determining the sequence $\hat{\mathbf{x}}_0$ by (19) for $n = 1, 2, \ldots, N$. Note that $\hat{\mathbf{x}}_0$ corresponds to interval C_0. Then, we consider $\phi = \theta_1$ and invert the decision symbol x_n, $n \in \{1, 2, \ldots, N\}$, which produced θ_1. This way, we obtain the new sequence $\hat{\mathbf{x}}_1$ that corresponds to C_1. We continue by considering $\phi = \theta_2$ and repeating the above procedure to obtain $\hat{\mathbf{x}}_2$ that corresponds to C_2. Subsequently, we set $\phi = \theta_3$ to obtain $\hat{\mathbf{x}}_3$ and continue similarly with $\phi = \theta_4, \theta_5, \ldots, \theta_{2N-1}$ to determine all $2N$ sequences $\hat{\mathbf{x}}_0, \hat{\mathbf{x}}_1, \ldots, \hat{\mathbf{x}}_{2N-1}$. Then, we compare them against the metric of interest in (16) to identify the optimal one which is $\hat{\mathbf{x}}^{\mathrm{ML}}$.

The proposed algorithm that we just described is presented in Fig. 1.[6] The overall complexity to produce the $2N$ sequences $\hat{\mathbf{x}}_0, \hat{\mathbf{x}}_1, \ldots, \hat{\mathbf{x}}_{2N-1}$ among which is $\hat{\mathbf{x}}^{\mathrm{ML}}$ is dominated by the computational cost of the sorting operation in (21) which is on the order of $\mathcal{O}(2N\log_2 2N) = \mathcal{O}(N\log N)$.

Improvements to the proposed algorithm: We can simplify the algorithm that we described above by taking into account a few properties of the generated candidate sequences.

First, observe that the candidate sequence that we obtain at any $\phi \in [0, \pi)$ is the complement of the candidate sequence

[6] If $\phi_n^{(j)} = 0$ for some $j \in \{1, 2\}$ and $n \in \{1, 2, \ldots, N\}$, then $\theta_1 = 0$, implying that the candidate sequence $\hat{\mathbf{x}}_0$ cannot be defined at $\phi = 0$ due to sign ambiguity with respect to the symbol x_n that produced $\theta_1 = 0$. Then, we change the interval of ϕ from $[0, 2\pi)$ to $[\theta^*, 2\pi+\theta^*)$, where θ^* is a point that belongs to the interval that precedes $\theta_1 = 0$. In this case, we select θ^* to be the mid-point of the preceding interval $(\theta_{2N}, 2\pi)$, i.e., $\theta^* = \frac{\theta_{2N}-2\pi}{2}$, as shown at lines 6–10 of the algorithm in Fig. 1. Hence, $\theta_{2N} < \theta^* \pmod{2\pi}$ and $\theta^* < \theta_1 = 0$, implying that the first two intervals in (22) change to $C_0 = (\theta^*, \theta_1 = 0)$ and $C_1 = (\theta_1 = 0, \theta_2)$ where the corresponding two candidate sequences $\hat{\mathbf{x}}_0$ and $\hat{\mathbf{x}}_1$ are uniquely defined.

Finally, if $\phi_n^{(j)} = \phi_l^{(k)}$ for some $j, k \in \{1, 2\}$ and $n, l \in \{1, 2, \ldots, N\}$ with $n \neq l$, then $\theta_i = \theta_{i+1}$ for some $i \in \{1, 2, \ldots, 2N-1\}$, implying that interval $C_i = (\theta_i, \theta_{i+1})$ does not exist and must be removed from the list of $2N$ intervals in (22); the two adjacent intervals $C_{i-1} = (\theta_{i-1}, \theta_i = \theta_{i+1})$ and $C_{i+1} = (\theta_i = \theta_{i+1}, \theta_{i+2})$ that correspond to the candidate sequences $\hat{\mathbf{x}}_{i-1}$ and $\hat{\mathbf{x}}_{i+1}$ become successive and the total number of $2N$ intervals (and sequences) is reduced by one. In this case, we let the algorithm produce the invalid intermediate candidate sequence $\hat{\mathbf{x}}_i$ without increasing its complexity or affecting its optimality.

Algorithm 1 Optimal Noncoherent Binary Orthogonal Detection

Input: $\mathbf{y}_1,\ \mathbf{y}_2,\ \dots\ ,\mathbf{y}_N$

for $n = 1 : N$ **do**
  $\phi_n^{(1)} := +\frac{\pi}{2} + \underline{/y_n[1] - y_n[2]} \pmod{2\pi}$
  $\phi_n^{(2)} := -\frac{\pi}{2} + \underline{/y_n[1] - y_n[2]} \pmod{2\pi}$
end for
$(\theta_1, \theta_2, \dots, \theta_{2N}) := \mathsf{sort}\left(\phi_1^{(1)}, \phi_1^{(2)}, \phi_2^{(1)}, \phi_2^{(2)}, \dots, \phi_N^{(1)}, \phi_N^{(2)}\right)$
if $\theta_1 > 0$ **then**
  $\theta^* := 0$
else
  $\theta^* := \frac{\theta_{2N} - 2\pi}{2}$
end if
for $n = 1 : N$ **do**
  $\hat{x}_n := \arg\max(\Re\{\mathrm{e}^{-j\theta^*} y_n[1]\}, \Re\{\mathrm{e}^{-j\theta^*} y_n[2]\})$
end for
$\hat{\mathbf{x}}_0 := \hat{\mathbf{x}}$
for $i = 1 : 2N - 1$ **do**
  Invert in $\mathbf{x}$ the symbol decision $\hat{x}_n$ for which θ_i was obtained
  $\hat{\mathbf{x}}_i := \hat{\mathbf{x}}$
end for
$\hat{\mathbf{x}}^{\mathrm{ML}} := \arg\max_{\mathbf{x} \in \{\hat{\mathbf{x}}_0, \hat{\mathbf{x}}_1, \dots, \hat{\mathbf{x}}_{2N-1}\}} |y_1[x_1] + y_2[x_2] + \ldots + y_N[x_N]|$

Output: $\hat{\mathbf{x}}^{\mathrm{ML}}$

Fig. 1. Optimal noncoherent sequence detection algorithm for binary orthogonal modulation and zero-offset FM0 coding.

Algorithm 2 Optimal Noncoherent Binary Orthogonal Detection in Time $\mathcal{O}(N\log N)$

Input: $\mathbf{y}_1,\ \mathbf{y}_2,\ \dots\ ,\mathbf{y}_N$

1: **for** $n = 1 : N$ **do**
2:   $\phi_n := \frac{\pi}{2} + \underline{/y_n[1] - y_n[2]} \pmod{\pi}$
3: **end for**
4: $(\theta_1, \theta_2, \dots, \theta_N) := \mathsf{sort}(\phi_1, \phi_2, \dots, \phi_N)$
5: **if** $\theta_1 > 0$ **then**
6:   $\theta^* := 0$
7: **else**
8:   $\theta^* := \frac{\theta_N - \pi}{2}$
9: **end if**
10: **for** $n = 1 : N$ **do**
11:   $\hat{x}_n := \arg\max(\Re\{\mathrm{e}^{-j\theta^*} y_n[1]\}, \Re\{\mathrm{e}^{-j\theta^*} y_n[2]\})$
12: **end for**
13: $\hat{\mathbf{x}}^{\mathrm{comp}} := (\hat{\mathbf{x}})^{\mathrm{c}}$
14: $value\_\hat{\mathbf{x}} := y_1[\hat{x}_1] + y_2[\hat{x}_2] + \ldots + y_N[\hat{x}_N]$
15: $value\_\hat{\mathbf{x}}^{\mathrm{comp}} := y_1[\hat{x}_1^{\mathrm{comp}}] + y_2[\hat{x}_2^{\mathrm{comp}}] + \ldots + y_N[\hat{x}_N^{\mathrm{comp}}]$
16: $[\mathrm{ML}\_value, \hat{\mathbf{x}}_{\mathrm{best}}] := \max(|value\_\hat{\mathbf{x}}|, |value\_\hat{\mathbf{x}}^{\mathrm{comp}}|)$
17: $\hat{\mathbf{x}}^{\mathrm{ML}} := \hat{\mathbf{x}}_{\mathrm{best}}$
18: **for** $i = 1 : N - 1$ **do**
19:   let n be the index for which $\theta_i = \phi_n$ at line 4
20:   $value\_\hat{\mathbf{x}} := value\_\hat{\mathbf{x}} - y_n[\hat{x}_n] + y_n[\hat{x}_n^{\mathrm{comp}}]$
21:   $value\_\hat{\mathbf{x}}^{\mathrm{comp}} := value\_\hat{\mathbf{x}}^{\mathrm{comp}} - y_n[\hat{x}_n^{\mathrm{comp}}] + y_n[\hat{x}_n]$
22:   $\hat{x}_n^{\mathrm{comp}} := \hat{x}_n$
23:   $\hat{x}_n := \hat{x}_n^{\mathrm{c}}$
24:   $[best\_value, \hat{\mathbf{x}}_{\mathrm{best}}] := \max(|value\_\hat{\mathbf{x}}|, |value\_\hat{\mathbf{x}}^{\mathrm{comp}}|)$
25:   **if** $best\_value > \mathrm{ML}\_value$ **then**
26:     $\mathrm{ML}\_value := best\_value$
27:     $\hat{\mathbf{x}}^{\mathrm{ML}} := \hat{\mathbf{x}}_{\mathrm{best}}$
28:   **end if**
29: **end for**

Output: $\hat{\mathbf{x}}^{\mathrm{ML}}$

Fig. 2. Simplified optimal noncoherent sequence detection algorithm for binary orthogonal modulation and zero-offset FM0 coding with complexity $\mathcal{O}(N\log N)$.

that we obtain at $\phi + \pi$.[7] Indeed, for the decision rule in (19), we observe that, for any $\phi \in [0, \pi)$ and any $n = 1, 2, \dots, N$, we have

$$\cos\left(\phi - \underline{/y_n[1] - y_n[2]}\right) = -\cos\left((\phi + \pi) - \underline{/y_n[1] - y_n[2]}\right). \tag{23}$$

Hence, for any $\phi \in [0, \pi)$, (19) results in complementary sequences at ϕ and $\phi + \pi$.

Then, from (20), we observe that $\left|\phi_n^{(2)} - \phi_n^{(1)}\right| = \pi$, hence $\phi_n^{(1)}$ and $\phi_n^{(2)}$ result in complementary sequences. Moreover, one of them belongs to $[0, \pi)$ and the other one belongs to $[\pi, 2\pi)$. As a result,[8]

$$0 < \theta_1 < \theta_2 < \ldots < \theta_N < \pi < \theta_{N+1} < \ldots < \theta_{2N} < 2\pi \tag{24}$$

and

$$\hat{\mathbf{x}}_{n+N} = \hat{\mathbf{x}}_n^{\mathrm{c}}, \quad n = 0, 1, \dots, N - 1. \tag{25}$$

This implies that it suffices to identify the N candidate sequences at $[0, \theta_N)$ and, then, consider also their complements. Note that we ignore $[\theta_N, \pi)$ because it corresponds to the complementary sequence $\hat{\mathbf{x}}_0^{\mathrm{c}}$.

Similar observations were made in [37]–[41], [69], [70] in the context of PSK, where complementary sequences are equivalent with respect to the metric of interest. This is in contrast to FSK where complementary sequences have in general different metric. Hence, in this work, we have to store both complementary sequences for each interval, while searching for the optimal one.

The proposed algorithm (that includes the above improvements) is presented in Fig. 2. The N points of decision changes are computed at lines 1–3 and sorted at line 4. At lines 5–12, we identify the initial sequence $\hat{\mathbf{x}}$ that is optimal in C_0.[9] At lines 14 and 15, we evaluate the sum in (16) for sequences $\hat{\mathbf{x}}$ and $\hat{\mathbf{x}}^{\mathrm{c}}$, respectively. The two sums are compared against each other with respect to their magnitudes; the best value as well as the corresponding sequence are stored in ML_value and $\hat{\mathbf{x}}^{\mathrm{ML}}$ at lines 16 and 17, respectively. At lines 18–29, we examine $\theta_1, \theta_2, \dots, \theta_{N-1}$ serially to find the optimal sequence $\hat{\mathbf{x}}^{\mathrm{ML}}$. Specifically, at line 19, we move to the next θ_i in the sorted list, which was obtained from some received vector, say $\mathbf{y}_n$. At lines 20–23, we update the sums in (16) for sequences $\hat{\mathbf{x}}$ and $\hat{\mathbf{x}}^{\mathrm{c}}$ and the value of $\hat{x}_n$. At line 24, the two sums are compared against each other and the best one together with the corresponding sequence are stored in $best\_value$ and $\hat{\mathbf{x}}_{\mathrm{best}}$, respectively. If $best\_value$ is greater than the up-to-date ML_value, then we update ML_value and the optimal sequence $\hat{\mathbf{x}}^{\mathrm{ML}}$ at lines 26 and 27, respectively.

By inspection, the exact computational cost of the algorithm

[7] Since the constellation is binary, we use the term "complementary sequences" to indicate sequences $\mathbf{x}$ and $\mathbf{y}$ that are related by $\mathbf{y}^{\mathrm{c}} = \mathbf{x}$ (i.e., $y_n^{\mathrm{c}} = x_n$, $n = 1, 2, \dots, N$) where $1^{\mathrm{c}} = 2$ and $2^{\mathrm{c}} = 1$.

[8] Once more, we assume that $\theta_i < \theta_{i+1}$, for any $i = 1, 2, \dots, N - 1$, and $\theta_1 > 0$. The case where the above assumption does not hold is examined in Footnote 9.

[9] As in the algorithm of Fig. 1 (see Footnote 6), if $\phi_n^{(j)} = 0$ for some $j \in \{1, 2\}$ and $n \in \{1, 2, \dots, N\}$, i.e., $\theta_1 = 0$, then we compute $\hat{\mathbf{x}}_0$ at the mid-point θ^* of the interval that precedes $\theta_1 = 0$, i.e., $\theta^* = \frac{\theta_{2N} - 2\pi}{2}$. Since $\theta_{2N} = \theta_N + \pi$ due to (23) and (24), it turns out that $\theta^* = \frac{\theta_N - \pi}{2}$, as shown at line 8 of the algorithm in Fig. 2. Otherwise (that is, if $\phi_n^{(j)} \neq 0$ for any $j \in \{1, 2\}$ and $n \in \{1, 2, \dots, N\}$), θ_1 is nonzero and θ^* is set to zero, as shown at line 6 of the algorithm in Fig. 2.

Finally, if $\phi_n^{(j)} = \phi_l^{(k)}$ for some $j, k \in \{1, 2\}$ and $n, l \in \{1, 2, \dots, N\}$ with $n \neq l$, then $\theta_i = \theta_{i+1}$ for some $i \in \{1, 2, \dots, N - 1\}$. In this case, we act exactly as we did in the algorithm of Fig. 1 (see Footnote 6), i.e., we let the algorithm produce the invalid intermediate sequences $\hat{\mathbf{x}}_i$ and $\hat{\mathbf{x}}_i^{\mathrm{c}}$ without increasing its complexity or affecting its optimality.

of Fig. 2, if we count arithmetic operations,[10] equals

$$J_2(N) = N\log_2 N + 17N - 4. \tag{26}$$

Its complexity is dominated by the computational cost of the sorting operation at line 4 which is on the order of $\mathcal{O}(N\log N)$.

2) Optimal algorithm for $M \geq 2$: If we fix $\phi \in [0, 2\pi)$, then the innermost maximization in (18) splits into independent maximizations for any $n = 1, 2, \ldots, N$, as

$$\hat{x}_n = \arg\max_{x\in\mathcal{M}} \Re\left\{\mathsf{e}^{-j\phi} y_n[x]\right\}. \tag{27}$$

We observe that, for fixed ϕ, (27) is solved by selecting the largest value of $\Re\left\{\mathsf{e}^{-j\phi}\mathbf{y}_n\right\}$. As ϕ scans $[0, 2\pi)$, the decision $\hat{x}_n$ may change only when, for some $k, l \in \mathcal{M}$ with $k \neq l$,

$$\begin{aligned}
&\Re\left\{\mathsf{e}^{-j\phi} y_n[k]\right\} = \Re\left\{\mathsf{e}^{-j\phi} y_n[l]\right\} \\
\Leftrightarrow\ &\Re\left\{\mathsf{e}^{-j\phi}\left(y_n[k] - y_n[l]\right)\right\} = 0 \\
\Leftrightarrow\ &\cos\left(\phi - \angle y_n[k] - y_n[l]\right) = 0 \\
\Leftrightarrow\ &\phi = \underbrace{\pm\frac{\pi}{2} + \angle y_n[k] - y_n[l] \pmod{2\pi}}_{\phi^{(1)}_{n,\{k,l\}},\,\phi^{(2)}_{n,\{k,l\}}}.
\end{aligned} \tag{28}$$

Hence, as ϕ scans $[0, 2\pi)$, the decision on the sequence $\hat{\mathbf{x}}$ may change only at some of the points defined in (28), for any $k, l \in \mathcal{M}$ with $k \neq l$ and $n = 1, 2, \ldots, N$. Although (28) produces $2N\binom{M}{2} = M(M-1)N$ such points, it turns out that the decision $\hat{\mathbf{x}}$ changes at only (at most) $2(M-1)N$ points. This is stated in the following proposition.

Proposition 1: For $M \geq 2$, there exist at most $2(M-1)N$ changes of the sequence decision $\hat{\mathbf{x}}$ in the interval $[0, 2\pi)$.

Proof:

Since, for a given $\phi \in [0, 2\pi)$, the N maximizations in (18) are independent of each other, it suffices to restrict our attention to a single symbol x_n and show that the decision $\hat{x}_n$ changes at most $2(M-1)$ times in the interval $[0, 2\pi)$.

Consider first the interval $[0, \pi)$. As ϕ scans $[0, \pi)$, the decision $\hat{x}_n$ changes at K points given by (28), say $\phi_{n_1}, \phi_{n_2}, \ldots, \phi_{n_K}$, where, without loss of generality,[11]

$$0 < \phi_{n_1} < \phi_{n_2} < \ldots < \phi_{n_K} < \pi. \tag{29}$$

That is, the interval $[0, \pi)$ is partitioned into $K + 1$ successive intervals

$$C_{n_0} = (0, \phi_{n_1}),\ C_{n_1} = (\phi_{n_1}, \phi_{n_2}),\ \ldots,\ C_{n_K} = (\phi_{n_K}, \pi) \tag{30}$$

in such a way that the decision in favor of x_n *(i)* is constant in each interval and *(ii)* is different over successive intervals. Let $\hat{x}_{n_0}, \hat{x}_{n_1}, \ldots, \hat{x}_{n_K}$ be these $K + 1$ decisions on x_n.

Since the decision on x_n is made using (27), we define the metric function in (27) with respect to symbol x_n as

$$\mu_n(\phi; x) = \Re\{\mathsf{e}^{-j\phi} y_n[x]\}, \quad \phi \in [0, 2\pi), \quad x \in \mathcal{M}. \tag{31}$$

Consider now an arbitrary value of $k \in \{0, 1, 2, \ldots, K-1\}$. Since $\hat{x}_n = \hat{x}_{n_k}$ for any $\phi \in C_{n_k}$ and $\hat{x}_n = \hat{x}_{n_{k+1}}$ for any $\phi \in C_{n_{k+1}}$, it is implied that

$$\begin{aligned}
&\mu_n(\phi; \hat{x}_{n_k}) > \mu_n(\phi; \hat{x}_{n_{k+1}}), \text{ if } \phi \in C_{n_k}, \\
&\mu_n(\phi; \hat{x}_{n_k}) = \mu_n(\phi; \hat{x}_{n_{k+1}}), \text{ if } \phi = \phi_{n_{k+1}}, \\
&\mu_n(\phi; \hat{x}_{n_k}) < \mu_n(\phi; \hat{x}_{n_{k+1}}), \text{ if } \phi \in C_{n_{k+1}}.
\end{aligned} \tag{32}$$

The latter inequality will hold true as long as ϕ does not meet any value $\phi' \neq \phi_{n_{k+1}}$ such that $\mu_n(\phi'; \hat{x}_{n_k}) = \mu_n(\phi'; \hat{x}_{n_{k+1}})$. By (28), there is only one such a point, namely $\phi_{n_{k+1}} + \pi$, which, however, lies outside $[0, \pi)$. Hence,

$$\mu_n(\phi; \hat{x}_{n_k}) < \mu_n(\phi; \hat{x}_{n_{k+1}}), \quad \forall\phi \in (\phi_{n_{k+1}}, \pi). \tag{33}$$

Similarly, considering an arbitrary value of $k \in \{1, 2, \ldots, K\}$ and using the same arguments, we can show that

$$\mu_n(\phi; \hat{x}_{n_k}) < \mu_n(\phi; \hat{x}_{n_{k-1}}), \quad \forall\phi \in (0, \phi_{n_k}). \tag{34}$$

From (33), it is implied that $\hat{x}_{n_0}$, i.e., the decision in C_{n_0}, cannot reappear in any other interval among $C_{n_1}, C_{n_2}, \ldots, C_{n_K}$ in $[0, \pi)$. Similarly, from (34), it is implied that $\hat{x}_{n_K}$ appears only in C_{n_K}. Finally, for any $k = 1, 2, \ldots, K-1$, (33) and (34) imply that the decision $\hat{x}_{n_k}$ cannot appear in $(0, \phi_{n_k})$ or $(\phi_{n_{k+1}}, \pi)$. Hence, it appears only in $(\phi_{n_k}, \phi_{n_{k+1}})$, which is C_{n_k} in (30). Therefore, the $K + 1$ intervals in (30) correspond to distinct decisions, i.e., $\hat{x}_{n_k} \neq \hat{x}_{n_j}$ if $k, j \in \{0, 1, \ldots, K\}$ with $k \neq j$. Since there are at most M available values for x_n, we conclude that $K + 1 \leq M$, i.e.,

$$K \leq M - 1. \tag{35}$$

Consider now the interval $[\pi, 2\pi)$. If the decision $\hat{x}_n$ changes at K' points as ϕ scans $[\pi, 2\pi)$, then, we can similarly show that

$$K' \leq M - 1. \tag{36}$$

As ϕ scans the entire circle $[0, 2\pi)$, the decision $\hat{x}_n$ changes exactly $K + K'$ times. From (35) and (36), we obtain $K + K' \leq 2M - 2 = 2(M-1)$. That is, the decision $\hat{x}_n$ changes at most $2(M-1)$ times. Therefore, the sequence decision $\hat{\mathbf{x}}$ changes at most $2(M-1)N$ times. □

The above proposition states that it suffices to check at most $2(M-1)N$ points where the sequence decision changes. When the points have been determined, the remaining process resembles to the algorithm of case $M = 2$. Specifically, after the identification of the points that correspond to actual decision changes, we seek the sequence $\hat{\mathbf{x}}$ obtained at each point θ_i that gives the largest metric in (16). In the case of $M > 2$, sequence $\hat{\mathbf{x}}(\phi)$ is not necessarily complementary with $\hat{\mathbf{x}}(\phi + \pi)$ and, thus, we need to seek the optimal sequence within the entire interval $[0, 2\pi)$.

The proposed algorithm for optimal noncoherent M-ary orthogonal sequence detection is depicted in Fig. 3. By inspection, the exact computational cost of the algorithm, if we count arithmetic operations, is upper bounded by

$$\begin{aligned}
J_M(N) = &\ 2(M-1)N\ \log_2(2(M-1)N) \\
&+ M(M-1)N\ \log_2(M(M-1)) \\
&+ \left(\frac{1}{4}M^4 + \frac{1}{2}M^3 + \frac{35}{4}M^2 + \frac{1}{2}M - 5\right)N.
\end{aligned} \tag{37}$$

[10]Complex addition, subtraction, multiplication, and division, magnitude, angle, modulo, and maximization operations, and logical comparison account for a single arithmetic operation.

[11]We again assume that $\phi_{n_1} > 0$. If $\phi_{n_1} = 0$, then we let ϕ scan the interval $[\theta^*, \pi + \theta^*)$ where $\theta^* < 0$ is an appropriately selected point in the interval that precedes $\phi_{n_1} = 0$, as described in Footnote 6.

Algorithm 3 Optimal Noncoherent M-ary Orthogonal Detection in Time $\mathcal{O}(N\log N)$

Input: $\mathbf{y}_1,\ \mathbf{y}_2,\ \ldots,\mathbf{y}_N$

1: **for** $n = 1 : N$ **do**
2: $\quad\boldsymbol{\phi}_n := [\ ]$
3: $\quad\mathbf{S}_n := [\ ]$
4: $\quad$**for** $k, l \in \mathcal{M}$ such that $k \neq l$ **do**
5: $\quad\quad\phi_n^{(1)} := +\frac{\pi}{2} + \underline{/y_n[k] - y_n[l]}\pmod{2\pi}$
6: $\quad\quad\phi_n^{(2)} := -\frac{\pi}{2} + \underline{/y_n[k] - y_n[l]}\pmod{2\pi}$
7: $\quad\quad\boldsymbol{\phi}_n := [\boldsymbol{\phi}_n, \phi_n^{(1)}, \phi_n^{(2)}]$
8: $\quad\quad\mathbf{S}_n := [\mathbf{S}_n, \{k,l\}, \{k,l\}]$
9: $\quad$**end for**
10: **end for**
11: $\boldsymbol{\phi} := [\ ]$
12: $\mathbf{I} := [\ ]$
13: $\mathbf{S} := [\ ]$
14: **for** $n = 1 : N$ **do**
15: $\quad[\boldsymbol{\phi}_n,\ \text{sort\_indices}] := \mathsf{sort}(\boldsymbol{\phi}_n)$
16: $\quad\mathbf{S}_n := \mathbf{S}_n[\text{sort\_indices}]$
17: $\quad$**if** $\phi_n[1] > 0$ **then**
18: $\quad\quad\theta^* := 0$
19: $\quad$**else**
20: $\quad\quad\theta^* := \frac{\phi_n[M(M-1)] - 2\pi}{2}$
21: $\quad$**end if**
22: $\quad\hat{x}_n := \arg\max\left(\Re\left\{e^{-j\theta^*} y_n[1]\right\}, \Re\left\{e^{-j\theta^*} y_n[2]\right\}, \ldots, \Re\left\{e^{-j\theta^*} y_n[M]\right\}\right)$
23: $\quad m := \hat{x}_n$
24: $\quad j := 1$
25: $\quad$**while** $j \leq M(M-1)$ **do**
26: $\quad\quad j' := \max\{j, j+1, \ldots, M(M-1)\}$ such that $\phi_n[j'] = \phi_n[j]$
27: $\quad\quad$**if** $j' = j$ **then**
28: $\quad\quad\quad$**if** $m \in \mathcal{S}_n[j]$ **then**
29: $\quad\quad\quad\quad m :=$ the unique element of set $\mathcal{S}_n[j] \setminus \{m\}$
30: $\quad\quad\quad\quad\boldsymbol{\phi} := [\boldsymbol{\phi}, \phi_n[j]]$
31: $\quad\quad\quad\quad\mathbf{I} := [\mathbf{I}, n]$
32: $\quad\quad\quad\quad\mathbf{S} := [\mathbf{S}, \mathcal{S}_n[j]]$
33: $\quad\quad\quad$**end if**
34: $\quad\quad$**else**
35: $\quad\quad\quad\mathcal{P} := \bigcup_{i=j}^{j'} \mathcal{S}_n[i]$
36: $\quad\quad\quad$**if** $\mathcal{P} \cap \{m\} \neq \emptyset$ **then**
37: $\quad\quad\quad\quad$**if** $j' < M(M-1)$ **then**
38: $\quad\quad\quad\quad\quad\phi^* := \frac{\phi_n[j'] + \phi_n[j'+1]}{2}$
39: $\quad\quad\quad\quad$**else**
40: $\quad\quad\quad\quad\quad\phi^* := \frac{\phi_n[M(M-1)] - 2\pi}{2}$
41: $\quad\quad\quad\quad$**end if**
42: $\quad\quad\quad\quad m' := \arg\max\left(\Re\left\{e^{-j\phi^*} y_n[1]\right\}, \Re\left\{e^{-j\phi^*} y_n[2]\right\}, \ldots, \Re\left\{e^{-j\phi^*} y_n[M]\right\}\right)$
43: $\quad\quad\quad\quad\boldsymbol{\phi} := [\boldsymbol{\phi}, \phi_n[j']]$
44: $\quad\quad\quad\quad\mathbf{I} := [\mathbf{I}, n]$
45: $\quad\quad\quad\quad\mathbf{S} := [\mathbf{S}, \{m, m'\}]$
46: $\quad\quad\quad\quad m := m'$
47: $\quad\quad\quad$**end if**
48: $\quad\quad$**end if**
49: $\quad\quad j := j' + 1$
50: $\quad$**end while**
51: **end for**
52: $[\boldsymbol{\theta},\ \text{sort\_indices}] := \mathsf{sort}(\boldsymbol{\phi})$
53: $\mathbf{I} := \mathbf{I}[\text{sort\_indices}]$
54: $\mathbf{S} := \mathbf{S}[\text{sort\_indices}]$
55: $\hat{\mathbf{x}}^{\text{ML}} := \hat{\mathbf{x}}$
56: $\mathit{value\_}\hat{\mathbf{x}} := y_1[\hat{x}_1] + y_2[\hat{x}_2] + \ldots + y_N[\hat{x}_N]$
57: $\text{ML\_}\mathit{value} := |\mathit{value\_}\hat{\mathbf{x}}|$
58: **for** $i = 1 : \mathsf{length}(\boldsymbol{\theta})$ **do**
59: $\quad n := I[i]$
60: $\quad m := \hat{x}_n$
61: $\quad m' :=$ the unique element of set $\mathcal{S}[i] \setminus \{m\}$
62: $\quad\mathit{value\_}\hat{\mathbf{x}} := \mathit{value\_}\hat{\mathbf{x}} - y_n[m] + y_n[m']$
63: $\quad\hat{x}_n := m'$
64: $\quad\mathit{best\_value} := |\mathit{value\_}\hat{\mathbf{x}}|$
65: $\quad$**if** $\mathit{best\_value} > \text{ML\_}\mathit{value}$ **then**
66: $\quad\quad\text{ML\_}\mathit{value} := \mathit{best\_value}$
67: $\quad\quad\hat{\mathbf{x}}^{\text{ML}} := \hat{\mathbf{x}}$
68: $\quad$**end if**
69: **end for**

Output: $\hat{\mathbf{x}}^{\text{ML}}$

Fig. 3. Optimal noncoherent sequence detection algorithm for M-ary orthogonal modulation with complexity $\mathcal{O}(N\log N)$.

The overall complexity of the algorithm is dominated by the sorting operation at line 52 and, thus, the worst-case complexity of the algorithm is $\mathcal{O}(2(M-1)N\log_2 2(M-1)N) = \mathcal{O}(N\log N)$.

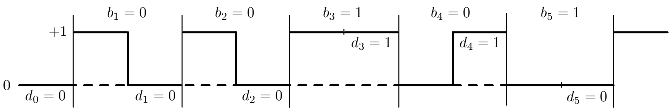

Fig. 4. Transmitted waveform in zero-offset FM0 coding.

III. Zero-offset FM0 Coding

FM0 (also called biphase-space or differential biphase coding [46]) is a line-coding technique that is used in the current RFID communications standard. In zero-offset FM0, the signal level can take two possible values; namely, 0 and 1. Specifically, the level changes at the middle of the bit period for bit 0, whereas for bit 1 it remains constant. Moreover, it always changes at the beginning of every bit period, as can been seen in Fig. 4, and, thus, the signals from one bit interval to another are not independent (i.e., FM0 induces memory). As a result, four possible transmitted waveforms can be generated which are depicted in Fig. 4 and can be represented in vector form as $[0\ 0]^T$, $[0\ 1]^T$, $[1\ 0]^T$, and $[1\ 1]^T$.

Consider, for example, the transmission of the nth information bit during the nth period. We denote by $d_n \in \{0,1\}$ the signal level at the end of nth bit period. Then, the signal level d_{n-1} at the end of the preceding period will change to d_{n-1}^{c} during the first half of the nth period.[12] For the second half, it will change to $d_n = d_{n-1}$ if the information bit is 0, or it will remain $d_n = d_{n-1}^{\text{c}}$ if the information bit is 1. This can be compactly expressed as

$$d_n = d_{n-1} \oplus b_n, \quad n = 1, 2, \ldots, N, \tag{38}$$

where $\oplus$ denotes exclusive-OR operation. Hence, during the nth bit period, the signal level takes the values $(d_{n-1}^{\text{c}},\ \underbrace{d_{n-1} \oplus b_n}_{d_n})$.

Assuming a sequence of N information bits $b_1, b_2, \ldots, b_N \in \{0,1\}$, the corresponding transmitted sequence is

$$\xrightarrow{} d_0 \;\Big|\; \overbrace{d_0^{\text{c}} \;\Big|\; \underbrace{d_0 \oplus b_1}_{d_1}}^{\text{bit } b_1} \;\Big|\; \overbrace{d_1^{\text{c}} \;\Big|\; \underbrace{d_1 \oplus b_2}_{d_2}}^{\text{bit } b_2} \;\Big|\; \overbrace{d_2^{\text{c}} \;\Big|\; \underbrace{d_2 \oplus b_3}_{d_3}}^{\text{bit } b_3} \;\Big|\; \ldots$$
$$\ldots \;\Big|\; \overbrace{d_{N-1}^{\text{c}} \;\Big|\; \underbrace{d_{N-1} \oplus b_N}_{d_N}}^{\text{bit } b_N} \;\Big|\; d_N^{\text{c}} \xleftarrow{} \tag{39}$$

or, in vector form,

$$\left[d_0, d_0^{\text{c}}, d_1, d_1^{\text{c}}, \ldots, d_N, d_N^{\text{c}}\right]^T = \underbrace{\begin{bmatrix} \mathbf{e}_{d_0} \\ \mathbf{e}_{d_1} \\ \vdots \\ \mathbf{e}_{d_N} \end{bmatrix}}_{\mathbf{d}} \tag{40}$$

[12] In this section, signal values 0 and 1 are considered complementary, i.e., $0^{\text{c}} = 1$ and $1^{\text{c}} = 0$.

where

$$d_0 \in \{0, 1\}, \tag{41}$$

$$d_n = d_{n-1} \oplus b_n = d_0 \oplus b_1 \oplus b_2 \oplus \ldots \oplus b_n, \quad n = 1, 2, \ldots, N, \tag{42}$$

$$\mathbf{e}_0 = \left[\begin{smallmatrix}0\\1\end{smallmatrix}\right], \quad \mathbf{e}_1 = \left[\begin{smallmatrix}1\\0\end{smallmatrix}\right]. \tag{43}$$

Hence, zero-offset FM0 coding is equivalent to differential BFSK modulation. For instance, if $b_1 = 0$, $b_2 = 0$, $b_3 = 1$, $b_4 = 0$, and $b_5 = 1$ and we use zero-offset FM0 coding with $d_0 = 0$, then we obtain $d_1 = 0$, $d_2 = 0$, $d_3 = 1$, $d_4 = 1$, and $d_5 = 0$, resulting in the waveform of Fig. 4.

The transmitted vector is $\sqrt{P}\mathbf{d}$ where P is the signal strength. Upon transmission over a flat-fading channel whose coherence time spans at least $N+1$ symbols [46], [50], [51], [55], the received vector is

$$\mathbf{y} = \begin{bmatrix}\mathbf{y}_0\\ \mathbf{y}_1\\ \vdots\\ \mathbf{y}_N\end{bmatrix} = \sqrt{P}h\mathbf{d} + \begin{bmatrix}\mathbf{w}_0\\ \mathbf{w}_1\\ \vdots\\ \mathbf{w}_N\end{bmatrix} \tag{44}$$

where $\mathbf{y}_n = \sqrt{P}h\mathbf{e}_{d_n} + \mathbf{w}_n$, $n = 0, 1, \ldots, N$, h is the complex channel coefficient, and $\mathbf{w}_0$, $\mathbf{w}_1$, $\ldots$, $\mathbf{w}_N$ is a sequence of independent and identically distributed 2×1 vectors that represent zero-mean additive white circularly symmetric complex Gaussian noise, i.e., $\mathbf{w}_n \sim \mathcal{CN}(\mathbf{0}, \sigma_w^2\mathbf{I}_2)$, $n = 0, 1, \ldots, N$.

The optimal noncoherent zero-offset FM0 sequence detector maximizes the conditional pdf of $\mathbf{y}$ given $\mathbf{d}$, that is,

$$\hat{\mathbf{d}}^{\mathrm{ML}} = \underset{\mathbf{d} \in \mathcal{I}_2^{N+1}}{\arg\max} \, f(\mathbf{y}|\mathbf{d}). \tag{45}$$

The optimization problem in (45) is equivalent to optimal noncoherent BFSK detection of (9). Hence, for Rayleigh fading (i.e., $h \sim \mathcal{CN}(0, \sigma_h^2)$) [50], [51], [55], from (15) we obtain

$$\hat{\mathbf{d}}^{\mathrm{ML}} = \underset{\mathbf{d} \in \mathcal{I}_2^{N+1}}{\arg\max} \, |\mathbf{d}^T\mathbf{y}|. \tag{46}$$

As with BFSK, (46) also offers GLRT-optimal sequence detection when the channel is non-Rayleigh or unknown. To find the optimal solution in (46), the algorithm for BFSK, presented in Fig. 2, can be directly employed to the sequence of received vectors $\mathbf{y}_0, \mathbf{y}_1, \ldots, \mathbf{y}_N$ to obtain the sequence $\hat{\mathbf{d}}^{\mathrm{ML}}$ with complexity $\mathcal{O}((N+1)\log(N+1)) = \mathcal{O}(N\log N)$. Finally, after identification of the optimal sequence $\hat{\mathbf{d}}^{\mathrm{ML}}$, the optimal information data sequence $\hat{\mathbf{b}}^{\mathrm{ML}}$ is obtained by plain differential decoding, i.e.,

$$\hat{b}_n^{\mathrm{ML}} = \hat{d}_n^{\mathrm{ML}} \oplus \hat{d}_{n-1}^{\mathrm{ML}}, \quad n = 1, 2, \ldots, N. \tag{47}$$

IV. ANTIPODAL FM0 CODING

A. Signal Model and Optimal Sequence Detection

In antipodal FM0 coding, the transmission process adopts the same principles as in zero-offset FM0 coding. The only difference is that the signal level takes the values 1 and -1 (instead of 0 and 1). The four possible transmitted waveforms are depicted in Fig. 5 and can be represented in vector form as $[1\ 1]^T$, $[1\ -1]^T$, $[-1\ 1]^T$, and $[-1\ -1]^T$.

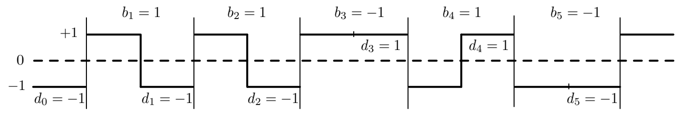

Fig. 5. Transmitted waveform in antipodal FM0 coding.

Similarly to zero-offset FM0 coding, it is straightforward to show that $d_n = d_{n-1}b_n$. Hence, during the nth bit period, the signal level takes the values $(-d_{n-1}, \underbrace{d_{n-1}b_n}_{d_n})$. For a sequence of N information bits $b_1, b_2, \ldots, b_N \in \{\pm 1\}$, the corresponding transmitted sequence is

$$\xrightarrow{\quad} d_0 \;\Big|\; \overbrace{-d_0 \;\Big|\; \underbrace{d_0 b_1}_{d_1}}^{\text{bit } b_1} \;\Big|\; \overbrace{-d_1 \;\Big|\; \underbrace{d_1 b_2}_{d_2}}^{\text{bit } b_2} \;\Big|\; \overbrace{-d_2 \;\Big|\; \underbrace{d_2 b_3}_{d_3}}^{\text{bit } b_3} \;\Big|\; \ldots$$

$$\ldots \;\Big|\; \overbrace{-d_{N-1} \;\Big|\; \underbrace{d_{N-1} b_N}_{d_N}}^{\text{bit } b_N} \;\Big|\; -d_N \xleftarrow{\quad} \tag{48}$$

or, in vector form,

$$\left[d_0, -d_0, d_1, -d_1, \ldots, d_N, -d_N\right]^T = \underbrace{\begin{bmatrix}d_0\\ d_1\\ \vdots\\ d_N\end{bmatrix}}_{\mathbf{d}} \otimes \begin{bmatrix}1\\ -1\end{bmatrix} \tag{49}$$

where

$$d_0 \in \{\pm 1\}, \tag{50}$$

$$d_n = d_{n-1}b_n = d_0 b_1 b_2 \ldots b_n, \quad n = 1, 2, \ldots, N, \tag{51}$$

and $\otimes$ denotes Kronecker-product operation. Hence, antipodal FM0 coding is equivalent to differential antipodal modulation, as shown in [46]. For instance, if $b_1 = +1, b_2 = +1, b_3 = -1, b_4 = +1$, and $b_5 = -1$ and we use antipodal FM0 line coding with $d_0 = -1$, then we obtain $d_1 = -1, d_2 = -1, d_3 = +1, d_4 = +1$, and $d_5 = -1$, resulting in the waveform of Fig. 5.

The transmitted signal vector is $\sqrt{\frac{P}{2}}\mathbf{d} \otimes \begin{bmatrix}1\\ -1\end{bmatrix}$ where P is the signal strength. Upon transmission over a flat-fading channel whose coherence time spans at least $N+1$ symbols, the optimal (coherent or noncoherent) detector correlates the downconverted received sequence with the pulse $\begin{bmatrix}1\\ -1\end{bmatrix}$ at the bit rate (with an offset by half bit period to match the corresponding transmitted sequence), resulting in the $(N+1) \times 1$ vector

$$\mathbf{y} = \begin{bmatrix}y_0\\ y_1\\ \vdots\\ y_N\end{bmatrix} = \sqrt{P}h\mathbf{d} + \mathbf{w} \tag{52}$$

where h is the complex channel coefficient and $\mathbf{w} \sim \mathcal{CN}(\mathbf{0}, \sigma_w^2\mathbf{I}_{N+1})$ denotes zero-mean additive white circularly symmetric complex Gaussian noise.

The optimal noncoherent antipodal FM0 sequence detector maximizes the conditional pdf of $\mathbf{y}$ given $\mathbf{d}$, that is,

$$\hat{\mathbf{d}}^{\mathrm{ML}} = \underset{\mathbf{d}\in\{\pm 1\}^{N+1}}{\arg\max}\ f\left(\mathbf{y}|\mathbf{d}\right). \tag{53}$$

It can be shown that, for Rayleigh fading, the ML sequence detection optimization problem can be expressed as

$$\hat{\mathbf{d}}^{\mathrm{ML}} = \underset{\mathbf{d}\in\{\pm 1\}^{N+1}}{\arg\max}\ |\mathbf{d}^T\mathbf{y}| \tag{54}$$

by following the same derivation steps as in Section II-A (eq's (8)–(15)). For non-Rayleigh or unknown channel, the GLRT rule for antipodal FM0 coding admits the same optimization problem, i.e.,

$$\hat{\mathbf{d}}^{\mathrm{GLRT}} = \underset{\mathbf{d}\in\{\pm 1\}^{N+1}}{\arg\max}\ |\mathbf{d}^T\mathbf{y}| \tag{55}$$

by following the same derivation as in eq. (17). After identification of the optimal sequence $\hat{\mathbf{d}}^{\mathrm{ML}}$, the optimal information data sequence $\hat{\mathbf{b}}^{\mathrm{ML}}$ is obtained by plain differential decoding, i.e.,

$$\hat{b}_n^{\mathrm{ML}} = \hat{d}_n^{\mathrm{ML}}\hat{d}_{n-1}^{\mathrm{ML}}, \quad n = 1, 2, \ldots, N. \tag{56}$$

B. Log-linear-complexity Optimal Detection

An efficient algorithm that computes the solution of (55) with log-linear complexity was developed in [37], [38].[13] For completeness, we present it shortly in this subsection.

As in the development of the optimal algorithm for BFSK detection (Section II-B), we use the fact that

$$\begin{aligned}
&\max_{\mathbf{d}\in\{\pm 1\}^{N+1}}\left|\mathbf{d}^T\mathbf{y}\right| = \max_{\mathbf{d}\in\{\pm 1\}^{N+1}}|d_0y_0 + d_1y_1 + \ldots + d_Ny_N| \\
&= \max_{\mathbf{d}\in\{\pm 1\}^{N+1}}\ \max_{\phi\in[0,2\pi)} \Re\left\{\mathsf{e}^{-j\phi}\left(d_0y_0 + d_1y_1 + \ldots + d_Ny_N\right)\right\} \\
&= \max_{\phi\in[0,2\pi)}\ \max_{\mathbf{d}\in\{\pm 1\}^{N+1}} \Big\{d_0\Re\left\{\mathsf{e}^{-j\phi}y_0\right\} + d_1\Re\left\{\mathsf{e}^{-j\phi}y_1\right\} + \ldots \\
&\qquad\qquad \ldots + d_N\Re\left\{\mathsf{e}^{-j\phi}y_N\right\}\Big\}.
\end{aligned} \tag{57}$$

For a given point $\phi\in[0,2\pi)$, the inner maximization in (57) is separable for each d_n and, thus, splits into independent maximizations for any $n = 0, 1, \ldots, N$, as

$$\begin{aligned}
&\hat{d}_n = \underset{d_n\in\{\pm 1\}}{\arg\max}\, d_n\Re\left\{\mathsf{e}^{-j\phi}y_n\right\} \\
&\Leftrightarrow \Re\left\{\mathsf{e}^{-j\phi}y_n\right\} \underset{\hat{d}_n=-1}{\overset{\hat{d}_n=+1}{\gtrless}} -\Re\left\{\mathsf{e}^{-j\phi}y_n\right\} \\
&\Leftrightarrow \Re\left\{\mathsf{e}^{-j\phi}y_n\right\} \underset{\hat{d}_n=-1}{\overset{\hat{d}_n=+1}{\gtrless}} 0 \Leftrightarrow \cos\!\left(\phi - \angle y_n\right) \underset{\hat{d}_n=-1}{\overset{\hat{d}_n=+1}{\gtrless}} 0.
\end{aligned} \tag{58}$$

According to (58), as ϕ scans $[0,2\pi)$, the decision $\hat{d}_n$ changes only when

$$\phi = \pm\frac{\pi}{2} + \angle y_n \pmod{2\pi}. \tag{59}$$

For any $\phi\in[0,\pi)$, we observe that the candidate sequences that we obtain at ϕ and $\phi+\pi$ are opposite, since $\cos\left(\phi - \angle y_n\right) = -\cos\left(\phi + \pi - \angle y_n\right)$, $n = 0, 1, \ldots, N$, in (58). Since opposite sequences result in the same metric value in (54), it suffices to restrict our search in $\phi\in[0,\pi)$. Hence, we keep the $N+1$ points in (59) that belong to $[0,\pi)$ and define them as

$$\phi_n = \frac{\pi}{2} + \angle y_n \pmod{\pi}, \quad n = 0, 1, \ldots, N. \tag{60}$$

Subsequently, we sort the $N+1$ points through[14]

$$\left(\theta_0, \theta_1, \ldots, \theta_N\right) = \mathsf{sort}\left(\phi_0, \phi_1, \ldots, \phi_N\right). \tag{61}$$

Then, the decision $\hat{\mathbf{d}}$ remains constant in each one of the $N+1$ intervals

$$C_0 = (0, \theta_0),\ C_1 = (\theta_0, \theta_1),\ \ldots,\ C_N = (\theta_{N-1}, \theta_N). \tag{62}$$

We note that we ignore the interval (θ_N, π) because it corresponds to the opposite sequence of the one in C_0.

Our objective now becomes the identification of the $N+1$ candidate sequences

$$\hat{\mathbf{d}}_0, \hat{\mathbf{d}}_1, \ldots, \hat{\mathbf{d}}_N \tag{63}$$

that are associated with the intervals $C_0, C_1, \ldots, C_N$, respectively, in $[0, \theta_N)$. We observe that sequences that correspond to adjacent intervals differ in exactly one element. For example, $\hat{\mathbf{d}}_0$ and $\hat{\mathbf{d}}_1$ differ in the element that produced θ_0. Hence, we propose to *(i)* identify $\hat{\mathbf{d}}_0$ at $\phi = 0$ through (58) and *(ii)* successively visit the angles $\theta_0, \ldots, \theta_{N-1}$ to produce the remaining N sequences, evaluate their metric in (54), and track the best sequence and its metric. Note that, at each point θ_i, the new sequence $\hat{\mathbf{d}}_{i+1}$ is produced with constant complexity by changing only one element of the preceding sequence $\hat{\mathbf{d}}_i$. The metric of $\hat{\mathbf{d}}_{i+1}$ is obtained with constant complexity by simply updating the metric of $\hat{\mathbf{d}}_i$ with respect to the single element that changed at θ_i.

The optimal algorithm for ML sequence detection of antipodal FM0 is illustrated in Fig. 6. The overall complexity is dominated by the computational cost of the sorting operation at line 4 which is on the order of $\mathcal{O}((N+1)\mathsf{log}_2(N+1)) = \mathcal{O}(N\mathsf{log}N)$.

Comparing the two algorithms in Figs. 2 and 6, we observe that the second one constructively builds and compares N sequences, instead of $2N$ sequences that are built by the first algorithm. This happens because the algorithm in Fig. 2 has to track both a candidate sequence $\hat{\mathbf{x}}$ and its complementary sequence $\hat{\mathbf{x}}^{\mathrm{c}}$. These two sequences have different metrics, as explained in Section II-B1. On the contrary, the algorithm in Fig. 6 calculates the metric of only half of the $2N$ sequences and avoids examining their opposite ones, since opposite sequences result in the same metric value in (54).

[13] The algorithm of [37], [38] reappeared in [41]. The principles of the algorithm in [37], [38] were followed also in [69] to develop a quadratic-complexity optimal algorithm.

[14] Again, we assume that $\phi_n \neq \phi_l$ and $\phi_n \neq 0$ for any $n, l \in \{0, 1, \ldots, N\}$ with $n \neq l$. If $\phi_n = 0$ for some $n \in \{0, 1, \ldots, N\}$, then we modify our search to the interval $[\theta^*, \pi + \theta^*)$, where $\theta^* = \frac{\theta_N - \pi}{2} < 0$, exactly as we did in Footnote 9 for the algorithm of Fig. 2. Finally, if $\phi_n = \phi_l$ for some $n, l \in \{0, 1, \ldots, N\}$ with $n \neq l$, then we let the algorithm produce an invalid intermediate sequence without increasing its complexity or affecting its optimality, exactly as we did in Footnote 9 for the algorithm of Fig. 2.

Algorithm 4 Optimal Noncoherent Antipodal FM0 Decoding in Time $\mathcal{O}(N\log N)$

Input: $y_0,\ y_1,\ \ldots\ ,y_N$

1: **for** $n = 0 : N$ **do**
2: $\quad\phi_n := \frac{\pi}{2} + \underline{/y_n} \pmod{\pi}$
3: **end for**
4: $(\theta_0, \theta_1, \ldots, \theta_N) := \mathsf{sort}\,(\phi_0, \phi_1, \ldots, \phi_N)$
5: **if** $\theta_0 > 0$ **then**
6: $\quad\theta^* := 0$
7: **else**
8: $\quad\theta^* := \frac{\theta_N - \pi}{2}$
9: **end if**
10: **for** $n = 0 : N$ **do**
11: $\quad\hat{d}_n := \mathsf{sign}\left(\Re\left\{\mathrm{e}^{-j\theta^*} y_n\right\}\right)$
12: **end for**
13: $\hat{\mathbf{d}}^{\mathrm{ML}} := \hat{\mathbf{d}}$
14: $value\_\hat{\mathbf{d}} := \hat{d}_0 y_0 + \hat{d}_1 y_1 + \ldots + \hat{d}_N y_N$
15: $\mathrm{ML}\_value := \left|value\_\hat{\mathbf{d}}\right|$
16: **for** $i = 0 : N - 1$ **do**
17: $\quad$let n be the index for which $\theta_i = \phi_n$ at line 4
18: $\quad value\_\hat{\mathbf{d}} := value\_\hat{\mathbf{d}} - 2\hat{d}_n y_n$
19: $\quad\hat{d}_n := -\hat{d}_n$
20: $\quad$**if** $\left|value\_\hat{\mathbf{d}}\right| > \mathrm{ML}\_value$ **then**
21: $\quad\quad\mathrm{ML}\_value := \left|value\_\hat{\mathbf{d}}\right|$
22: $\quad\quad\hat{\mathbf{d}}^{\mathrm{ML}} := \hat{\mathbf{d}}$
23: $\quad$**end if**
24: **end for**

Output: $\hat{\mathbf{d}}^{\mathrm{ML}}$

Fig. 6. Optimal noncoherent sequence detection algorithm for antipodal FM0 coding with complexity $\mathcal{O}\left(N\log N\right)$.

V. Simulation Results

We consider BFSK transmissions through a Rayleigh flat-fading channel. In Fig. 7, we plot the bit error rate (BER) of the ML noncoherent sequence detector as a function of the received signal-to-noise ratio (SNR) which is given by

$$\mathrm{SNR} = \frac{P\sigma_h^2}{\sigma_w^2}, \tag{64}$$

for sequence length $N = 1, 2, 10,$ and 100.[15] Especially for the case of the noncoherent energy detector (i.e., $N = 1$), we also plot the theoretical expression for the BER in Rayleigh flat fading, given by [28]

$$\mathrm{BER} = \frac{1}{\mathrm{SNR} + 2}. \tag{65}$$

As a reference, we include the BER of the conventional ML coherent detector with perfect channel knowledge. We observe that, as the sequence length increases, the noncoherent detector approaches the coherent one in terms of BER. Moreover, the BER of the conventional energy detector (i.e., $N = 1$) is 3–5dB far from the coherent one; as the sequence length N increases, the BER gap decreases to zero.

To demonstrate the rate of convergence to coherent detection performance, in Fig. 8, we set the SNR to 10dB and plot the BER of the ML noncoherent detector as a function of the sequence length N. We include the BER of the ML coherent detector, as a reference. We note that the BER of the noncoherent scheme with $N = 100$ is nearly equal to the BER of the coherent one with perfect channel knowledge. In the same figure, we plot the computational cost of the ML noncoherent detector implemented by both the proposed algorithm and the conventional exhaustive-search approach, as

[15] Since the channel is Rayleigh distributed, the ML and GLRT noncoherent detectors coincide.

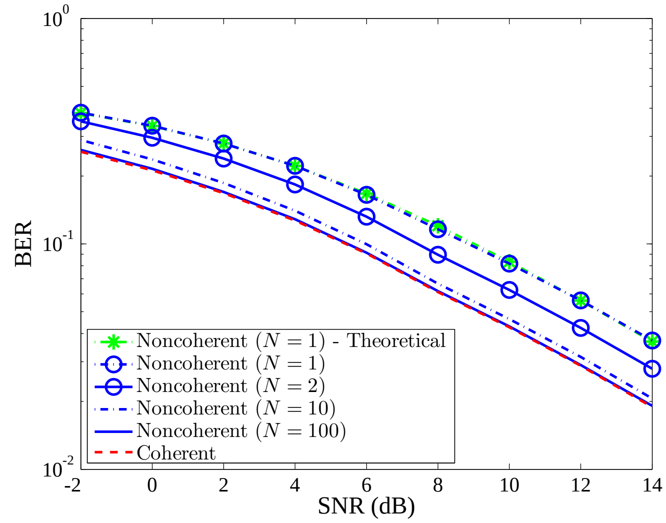

Fig. 7. BER versus bit SNR of ML/GLRT noncoherent BFSK detection with sequence length $N = 1, 2, 10, 100$ and ML coherent BFSK detection with perfect channel knowledge.

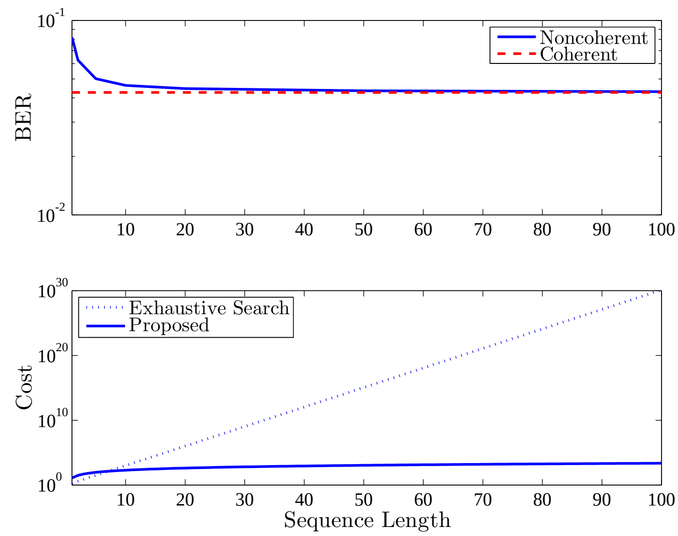

Fig. 8. BER and computational cost of ML/GLRT noncoherent BFSK detection versus sequence length N for SNR = 10dB.

a function of the sequence length N. We recall that the cost of the proposed algorithm equals $J_2(N)$, given by (26), while the cost of the conventional exhaustive-search approach is 2^N.

Finally, in Figs. 9 and 10, we repeat the above studies for 4FSK modulation and make similar observations for its symbol error rate (SER). In Fig. 9, for the case of the noncoherent energy detector (i.e., $N = 1$), the theoretical expression for the SER in Rayleigh flat fading is [28]

$$\mathrm{SER} = \frac{3}{\mathrm{SNR} + 2} - \frac{3}{2\mathrm{SNR} + 3} + \frac{1}{3\mathrm{SNR} + 4}. \tag{66}$$

For the complexity plot in Fig. 10, we recall that the cost of the proposed algorithm equals $J_4(N)$, given by (37), while the cost of the conventional exhaustive-search approach is 4^N. Once more, we observe that the SER of the noncoherent scheme with $N = 100$ is nearly equal to the SER of the

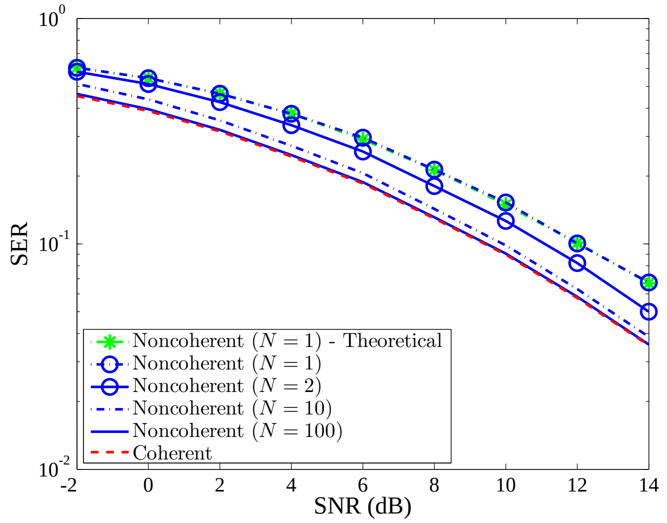

Fig. 9. SER versus symbol SNR of ML/GLRT noncoherent 4FSK detection with sequence length $N = 1, 2, 10, 100$ and ML coherent 4FSK detection with perfect channel knowledge.

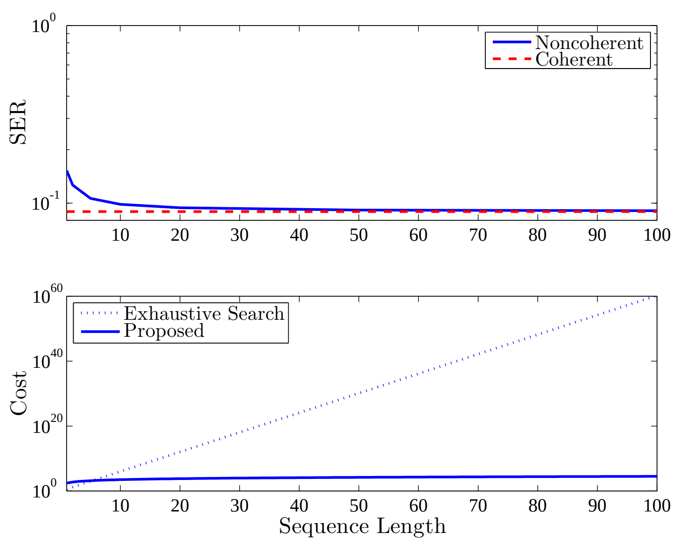

Fig. 10. SER and computational cost of ML/GLRT noncoherent 4FSK detection versus sequence length N for SNR = 10dB.

coherent one with perfect channel knowledge. Interestingly, this is achieved with $J_2(100) \simeq 2{,}360$ operations for BFSK and at most $J_4(100) \simeq 33{,}140$ operations for 4FSK (while the conventional exhaustive search is infeasible for such a sequence length since it would require $2^{100} \simeq 10^{30}$ and $4^{100} \simeq 10^{60}$, respectively, operations), opening avenues for practical deployments.

VI. Conclusions

For the first time in the literature, this work presented algorithms that perform optimal noncoherent sequence detection with log-linear (in the sequence length) complexity of orthogonally as well as FM0 modulated signals over flat fading. We demonstrated that, as the sequence length increases, the proposed detection schemes offer zero BER/SER performance gap compared to ML coherent detection. The above facts render the adoption of the proposed noncoherent sequence detection schemes for practical deployments as a probable option in the power-limited regime.

References

[1] L. Freitag, M. Stojanovic, and M. Johnson, “Analysis of channel effects on direct-sequence and frequency-hopped spread-spectrum acoustic communication,” *IEEE J. Ocean. Eng*, vol. 26, no. 4, pp. 586–593, Oct. 2001.

[2] F. Blackmon and L. Antonelli, “Remote, aerial, trans-layer, linear and non-linear downlink underwater acoustic communication,” in *Proc. IEEE OCEANS 2006*, Boston, MA, Sep. 2006.

[3] R. Jurdak, P. Aguiar, P. Baldi, and C. V. Lopes, “Software modems for underwater sensor networks,” in *Proc. IEEE OCEANS 2007*, Aberdeen, UK, Jun. 2007.

[4] Y. Li, X. Zhang, B. Benson, and R. Kastner, “Hardware implementation of symbol synchronization for underwater FSK,” in *Proc. IEEE SUTC 2010*, Newport Beach, CA, Jun. 2010, pp. 82–88.

[5] Y. Li, B. Benson, R. Kastner, and L. Chen, “A new hardware design scheme of symbol synchronization for an underwater acoustic receiver,” in *Third International Conference on Measuring Technology and Mechatronics Automation*, Shangshai, China, Jan. 2011, pp. 158–161.

[6] A. Sanchez, S. Blanc, P. Yuste, and J. J. Serrano, “A low cost and high efficient acoustic modem for underwater sensor networks,” in *Proc. IEEE OCEANS 2011*, Santander, Spain, Jun. 2011.

[7] C. Petrioli, R. Petroccia, J. Shusta, and L. Freitag, “From underwater simulation to at-sea testing using the ns-2 network simulator,” in *Proc. IEEE OCEANS 2011*, Santander, Spain, Jun. 2011.

[8] B. Zhang, Q. Zhan, S. Chen, M. Li, K. Ren, C. Wang, and D. Ma, “PriWhisper: Enabling keyless secure acoustic communication for smartphones,” *IEEE Internet Things J.*, vol. 1, no. 1, pp. 33–45, Feb. 2014.

[9] S. Chen, M. Li, Z. Qin, B. Zhang, and K. Ren, “AcousAuth: An acoustic-based mobile application for user authentication,” in *Proc. IEEE INFOCOM WKSHPS 2014*, Toronto, ON, May 2014, pp. 215–216.

[10] M. Kuba, M. Klatt, and A. Oeder, “Low-complexity sequence detection algorithm for FSK-based power line communications,” in *Proc. IEEE ISPLC 2014,* Glasgow, UK, Apr. 2014, pp. 150–155.

[11] A. R. Ndjiongue, H. C. Ferreira, K. Ouahada, and A. J. Han Vinckz, “Low-complexity SOCPBFSK-OOK interface between PLC and VLC channels for low data rate transmission applications,” in *Proc. IEEE ISPLC 2014,* Glasgow, UK, Apr. 2014, pp. 226–231.

[12] G. Vannucci, A. Bletsas, and D. Leigh, “A software-defined radio system for backscatter sensor networks,” *IEEE Trans. Wireless Commun.*, vol. 7, no. 6, pp. 2170–2179, Jun. 2008.

[13] J. Kimionis, A. Bletsas, and J. N. Sahalos, “Increased range bistatic scatter radio,” *IEEE Trans. Commun.*, vol. 62, no. 3, pp. 1091–1104, Mar. 2014.

[14] P. N. Alevizos, N. Fasarakis-Hilliard, K. Tountas, N. Agadakos, N. Kargas, and A. Bletsas, “Channel coding for increased range bistatic backscatter radio: Experimental results,” in *Proc. IEEE RFID-TA 2014*, Tampere, Finland, Sep. 2014.

[15] N. Fasarakis-Hilliard, P. N. Alevizos, and A. Bletsas, “Coherent detection and channel coding for bistatic scatter radio sensor networking,” *IEEE Trans. Commun.* vol. 63, no. 5, pp. 1798–1810, May 2015.

[16] P. N. Alevizos and A. Bletsas, “Noncoherent composite hypothesis testing receivers for extended range bistatic scatter radio WSNs,” in *Proc. IEEE ICC 2015*, London, UK, Jun. 2015, pp. 4448–4453.

[17] H. Okada and T. Itoh, “M-ary FSK modulation using short packet without a preamble and error detection codes for low power wireless communication,” *Wireless Sensor Network*, vol. 6, pp. 35–42, 2014.

[18] R. Annavajjala, P. C. Cosman, and L. B. Milstein, “On the performance of optimum noncoherent amplify-and-forward reception for cooperative diversity,” in *Proc. IEEE MILCOM 2005*, Atlantic City, NJ, Oct. 2005, pp. 3280–3288.

[19] D. Chen and J. N. Laneman, “Modulation and demodulation for cooperative diversity in wireless systems,” *IEEE Trans. Wireless Commun.*, vol. 5, no. 7, pp. 1785–1794, Jul. 2006.

[20] M. R. Souryal, “Non-coherent amplify-and-forward generalized likelihood ratio test receiver,” *IEEE Trans. Wireless Commun.*, vol. 9, no. 7, pp. 2320–2327, Jul. 2010.

[21] G. Farhadi and N. C. Beaulieu, “A low complexity receiver for noncoherent amplify-and-forward cooperative systems,” *IEEE Trans. Commun.*, vol. 58, no. 9, pp. 2499–2504, Sep. 2010.

[22] H. X. Nguyen, H. H. Nguyen, and T. Le-Ngoc, "Noncoherent receiver for amplify-and-forward relaying with M-FSK modulation," in *Proc. IEEE GLOBECOM 2011*, Houston, TX, Dec. 2011.

[23] P. Liu, S. Gazor, I.-M. Kim, and D. I. Kim, "Noncoherent amplify-and-forward cooperative networks: Robust detection and performance analysis," *IEEE Trans. Commun.*, vol. 61, no. 9, pp. 3644–3659, Jun. 2013.

[24] Y. Iwanami and P. H. Wittke, "Error performance analysis of an energy sequence estimation receiver for binary FSK on frequency-selective fading channels," *IEEE Trans. Wireless Commun.*, vol. 2, no. 2, pp. 260–269, Mar. 2003.

[25] I. Korn, J. P. Fonseka, and S. Xing, "Optimal binary communication with nonequal probabilities," *IEEE Trans. Commun.*, vol. 51, no. 9, pp. 1435–1438, Sep. 2003.

[26] S. Sharma, G. Yadav, and A. K. Chaturvedi, "Multicarrier on-off keying for fast frequency hopping multiple access systems in Rayleigh fading channels," *IEEE Trans. Wireless Commun.*, vol. 6, no. 3, pp. 769–774, Mar. 2007.

[27] M. C. Gursoy, "Error rate analysis for peaky signaling over fading channels," *IEEE Trans. Commun.*, vol. 57, no. 9, pp. 2546–2550, Sep. 2009.

[28] J. G. Proakis and M. Salehi, *Digital Communications*, 5th Ed. Upper Saddle River, NJ: Prentice-Hall, Nov. 2007.

[29] D. Warrier and U. Madhow, "Spectrally efficient noncoherent communication," *IEEE Trans. Inf. Theory,* vol. 48, no. 3, pp. 651–668, Mar. 2002.

[30] R.-R. Chen, R. Koetter, U. Madhow, and D. Agrawal, "Joint noncoherent demodulation and decoding for the block fading channel: A practical framework for approaching Shannon capacity," *IEEE Trans. Commun.*, vol. 51, no. 10, pp. 1676–1689, Oct. 2003.

[31] D. Makrakis and P. T. Mathiopoulos, "Optimal decoding in fading channels: A combined envelope, multiple differential and coherent detection approach," *in Proc. IEEE GLOBECOM 1989*, Dallas, TX, Nov. 1989, vol. 3, pp. 1551–1557.

[32] S. G. Wilson, J. Freebersyser, and C. Marshall, "Multi-symbol detection of M-DPSK," *in Proc. IEEE GLOBECOM 1989*, Dallas, TX, Nov. 1989, vol. 3, pp. 1692–1697.

[33] D. Divsalar and M. K. Simon, "Multiple-symbol differential detection of MPSK," *IEEE Trans. Commun.*, vol. 38, no. 3, pp. 300–308, Mar. 1990.

[34] H. Leib and S. Pasupathy, "Noncoherent block demodulation of PSK," in *Proc. IEEE VTC 1990*, Orlando, FL, May 1990, pp. 407–411.

[35] C.-D. Chung and F.-C. Hung, "Noncoherent maximum-likelihood block detection of orthogonal NFSK-LDPSK signals," *IEEE Trans. Vehic. Tech.*, vol. 51, no. 2, pp. 283–292, Mar. 2002.

[36] C.-D. Chung, "Coherent and differentially coherent detections of orthogonally multiplexed orthogonal phase-modulated signals," *IEEE Trans. Commun.*, vol. 51, no. 3, pp. 428–440, Mar. 2003.

[37] K. Mackenthun, "A fast algorithm for maximum likelihood detection of QPSK or π/4-QPSK sequences with unknown phase," in *Proc. IEEE PIMRC 1992*, Boston, MA, Oct. 1992, pp. 240–244.

[38] K. M. Mackenthun, Jr., "A fast algorithm for multiple-symbol differential detection of MPSK," *IEEE Trans. Commun.*, vol. 42, pp. 1471–1474, Feb./Mar./Apr. 1994.

[39] G. N. Karystinos and D. A. Pados, "Rank-2-optimal adaptive design of binary spreading codes," *IEEE Trans. Inf. Theory*, vol. 53, no. 9, pp. 3075–3080, Sep. 2007.

[40] D. S. Papailiopoulos, G. A. Elkheir, and G. N. Karystinos, "Maximum-likelihood noncoherent PAM detection," *IEEE Trans. Commun.*, vol. 61, no. 3, pp. 1152–1159, Mar. 2013.

[41] W. Sweldens, "Fast block noncoherent decoding," *IEEE Commun. Letters,* vol. 5, no. 4, pp. 132–134, Apr. 2001.

[42] I. Motedayen-Aval, A. Krishnamoorthy, and A. Anastasopoulos, "Optimal joint detection/estimation in fading channels with polynomial complexity," *IEEE Trans. Inf. Theory,* vol. 53, no. 1, pp. 209–223, Jan. 2007.

[43] I. Motedayen-Aval and A. Anastasopoulos, "Polynomial-complexity noncoherent symbol-by-symbol detection with application to adaptive iterative decoding of turbo-like codes," *IEEE Trans. Commun.*, vol. 51, no. 2, pp. 197–207, Feb. 2003.

[44] D. J. Ryan, I. B. Collings, and I. V. L. Clarkson, "GLRT-optimal noncoherent lattice decoding," *IEEE Trans. Signal. Proc.*, vol. 55, no. 7, pp. 3773–3786, Jul. 2007.

[45] R. G. McKilliam, D. J. Ryan, I. V. L. Clarkson, and I. B. Collings, "An improved algorithm for optimal noncoherent QAM detection," in *Proc. 2008 Australian Commun. Theory Workshop*, Christchurch, New Zealand, Feb. 2008, pp. 64–68.

[46] M. Simon and D. Divsalar, "Some interesting observations for certain line codes with application to RFID," *IEEE Trans. Commun.*, vol. 54, no. 4, pp. 583–586, Apr. 2006.

[47] C. Angerer, "Design and exploration of radio frequency identification systems by rapid prototyping," Ph.D. dissertation, Vienna University of Technology, Jul. 2010.

[48] M. Mohaisen, H. Yoon, and K. Chang, "Radio transmission performance of EPCglobal Gen-2 RFID system," in *Proc. IEEE ICACT 2008*, Gangwon-Do, South Korea, Dec. 2008, pp. 1423–1428.

[49] S. M. Yeo, B. Jeon, J. H. Bae, Y. J. Moon, Y. J. Kim, H. H. Roh, J. S. Park, Y. R. Seong, H. R. Oh, J. S. Kim, C. W. Park, and G. Y. Choi, "A channel allocation scheme considering with collisions and interferences in practical UHF RFID applied communication fields," in *Proc. IEEE RFID 2008*, Las Vegas, NV, Apr. 2008, pp. 258–268.

[50] R. Hoefel and D. Franco, "Joint performance and link budget analysis of HF RFID technology over fast and block fading channels," in *Proc. IEEE ICT 2009*, Marrakech, Morocco, May 2009, pp. 103–108.

[51] A. Lazaro, D. Girbau, and R. Villarino, "Effects of interferences in UHF RFID systems," *Progress In Electromagnetics Research*, vol. 98, pp. 425–443, 2009.

[52] C. Angerer, R. Langwieser, and M. Rupp, "RFID reader receivers for physical layer collision recovery," *IEEE Trans. Commun.*, vol. 58, no. 12, pp. 3526–3537, Dec. 2010.

[53] S. Thomas and M. S. Reynolds, "QAM backscatter for passive UHF RFID tags," in *Proc. IEEE RFID 2010*, Orlando, FL, Apr. 2010, pp. 210–214.

[54] Y. Yuan and D. Yu, "Reader planning in UHF RFID application," in *Proc. IEEE RFID-TA 2011*, Sitges, Spain, Sep. 2011, pp. 272–278.

[55] R. Morelos-Zaragoza, "On error performance improvements of passive UHF RFID systems via syndrome decoding," in *Proc. IEEE iThings/CPSCom 2011*, Dalian, China, Oct. 2011, pp. 127–130.

[56] J. Park and T.-J. Lee, "Channel-aware line code decision in RFID," *IEEE Commun. Lett.*, vol. 15, no. 12, pp. 1402–1404, Dec. 2011.

[57] A. Bletsas, J. Kimionis, A. G. Dimitriou, and G. N. Karystinos, "Single antenna coherent detection of collided FM0 RFID signals," *IEEE Trans. Commun.*, vol. 60, no. 3, pp. 756–766, Mar. 2012.

[58] R. Morelos-Zaragoza, "Unequal error protection with CRC-16 bits in EPC class-1 generation-2 UHF RFID systems," in *Proc. IEEE ISITA 2012*, Honolulu, HI, Oct. 2012, pp. 36–40.

[59] J. Park, J. Lee, H. Han, and T.-J. Lee, "Adaptive line code selection by identification efficiency for RFID systems," in *Proc. ACM ICUIMC 2012*, Kuala Lumpur, Malaysia, Feb. 2012, pp. 1–4.

[60] S.-B. Yim, J. Park, and T.-J. Lee, "Novel dynamic framed-slotted ALOHA using litmus slots in RFID systems," in *IEICE Trans. Commun.*, vol. E95-B, no. 4, pp. 1375–1383, Apr. 2012.

[61] S.-Y. Ahn, J.-S. Park, Y. R. Seong, and H.-R. Oh, "Performance evaluation of mobile RFID under multiple BoMR environments," in *Proc. IEEE ICUFN 2012*, Phuket, Thailand, Jul. 2012, pp. 484–489.

[62] Y. Yuan and D. Yu, "Nested error correcting code based highly reliable data reading for UHF RFID," in *Proc. IEEE RFID 2013*, Penang, Malaysia, May 2013, pp. 160–167.

[63] A. Schantin, "Iterative decoding of baseband and channel codes in a long-range RFID system," in *Proc. IEEE ICIT 2013*, Cape Town, South Africa, Feb. 2013, pp. 1671–1676.

[64] A. Schantin and C. Ruland, "Retransmission strategies for RFID systems using the EPC protocol," in *Proc. IEEE RFID-TA 2013*, Johor Bahru, Malaysia, Sep. 2013, pp. 1–6.

[65] J. G. Goh and S. V. Marić, "The capacities of frequency-hopped code-division multiple-access channels," *IEEE Trans. Inf. Theory,* vol. 44, no. 3, pp. 1204–1211, May 1998.

[66] C.-D. Chung, "Differential detection of quadrature frequency/phase modulated signals," *IEEE Trans. Commun.*, vol. 47, no. 4, pp. 546–557, Apr. 1999.

[67] S. H. Kim and S. W. Kim, "Frequency-hopped multiple-access communications with multicarrier on-off keying in Rayleigh fading channels," *IEEE Trans. Commun.,* vol. 48, no. 10, pp. 1692–1701, Oct. 2000.

[68] C. D. Meyer, *Matrix Analysis and Applied Linear Algebra*. Philadelphia, PA: SIAM, 2000.

[69] S. Gazor, M. Derakhtian, and A. A. Tadaion, "Computationally efficient maximum likelihood sequence estimation and activity detection for M-PSK signals in unknown flat fading channels," *IEEE Signal Process. Lett.,* vol. 17, no. 10, pp. 871–874, Oct. 2010.

[70] R. G. McKilliam, A. Pollok, B. Cowley, I. V. L. Clarkson, and B. G. Quinn, "Noncoherent least squares estimators of carrier phase and amplitude," in *Proc. IEEE ICASSP 2013*, Vancouver, BC, May 2013, pp. 4888–4892.

PLACE PHOTO HERE

Panos N. Alevizos (S'14) was born in Athens, Greece, in 1988. He received the Diploma and M.Sc. degrees in electronic and computer engineering from the Technical University of Crete (TUC), Greece, in 2012 and 2014, respectively. He is currently pursuing the Ph.D. degree at TUC.

Since 2012, he has been a Research Assistant with the Telecommunications Laboratory at TUC. His research interests include communication theory with emphasis on backscatter radio and RFID, wireless communications and networking, estimation and detection theory, information and coding theory, and probabilistic inference.

Mr. Alevizos is a Graduate Student Member of the IEEE Signal Processing Society. He is co-recipient of the 2015 IEEE International Conference on Acoustics, Speech, and Signal Processing (ICASSP) Best Student Paper Award.

PLACE PHOTO HERE

Yannis Fountzoulas (S'15) was born in Palermo, Italy, on February 13, 1988. He received the Diploma and M.Sc. degrees in electronic and computer engineering from the Technical University of Crete (TUC), Chania, Greece, in 2012 and 2014, respectively. He is currently working towards the Ph.D. degree at TUC.

Since 2013, he has been a Research Assistant with the Telecommunications Laboratory at TUC. His research interests are in the areas of communications and signal processing with an emphasis on low-complexity signal detection algorithms. He is co-recipient of the 2015 IEEE International Conference on Acoustics, Speech, and Signal Processing (ICASSP) Best Student Paper Award.

PLACE PHOTO HERE

George N. Karystinos (S'98-M'03) was born in Athens, Greece, on April 12, 1974. He received the Diploma degree in computer science and engineering (five-year program) from the University of Patras, Patras, Greece, in 1997 and the Ph.D. degree in electrical engineering from the State University of New York at Buffalo, Amherst, NY, in 2003.

From 2003 to 2005, he held an Assistant Professor position in the Department of Electrical Engineering, Wright State University, Dayton, OH. Since 2005, he has been with the Department of Electronic and Computer Engineering, Technical University of Crete, Chania, Greece, where he is presently an Associate Professor. His research interests are in the general areas of communication theory and signal processing with applications to signal waveform design, low-complexity sequence detection, backscatter communications and RFID, and large-scale MIMO systems.

Dr. Karystinos is a member of the IEEE Signal Processing, Communications, Information Theory, and Computational Intelligence Societies. For articles that he coauthored with students and colleagues, he received a 2001 IEEE International Conference on Telecommunications (ICT) best paper award, the 2003 IEEE Transactions on Neural Networks Outstanding Paper Award, the 2011 IEEE International Conference on RFID-Technologies and Applications (RFID-TA) Second Best Student Paper Award, the 2013 International Symposium on Wireless Communication Systems (ISWCS) Best Paper Award in Signal Processing and Physical Layer Communications, and the 2015 IEEE International Conference on Acoustics, Speech, and Signal Processing (ICASSP) Best Student Paper Award.

PLACE PHOTO HERE

Aggelos Bletsas (S'03-M'05-SM'14) received with excellence the Diploma degree in Electrical and Computer Engineering from the Aristotle University of Thessaloniki, Greece, in 1998 and the S.M. and Ph.D. degrees from the Massachusetts Institute of Technology in 2001 and 2005, respectively. He worked at Mitsubishi Electric Research Laboratories (MERL), Cambridge, MA, as a Postdoctoral Fellow and at Radiocommunications Laboratory (RCL), Department of Physics, Aristotle University of Thessaloniki, as a Visiting Scientist. He joined the School of Electronic and Computer Engineering, Technical University of Crete, in summer of 2009, as an Assistant Professor and was promoted to Associate Professor at the beginning of 2014.

His research interests span the broad area of scalable wireless communication and networking, with emphasis on relay techniques, backscatter communications and RFID, energy harvesting, radio hardware/software implementations for wireless transceivers and low-cost sensor networks. His current vision and focus is on single-transistor front-ends and backscatter sensor networks for LARGE-scale environmental sensing. He is the principal investigator (PI) of project BLASE: Backscatter Sensor Networks for Large-Scale Environmental Sensing, funded from the General Secretariat of Research & Technology Action Proposals evaluated positively from the 3rd European Research Council (ERC) Call. He is also Management Committee (MC) member and National Representative in the European Union COST Action IC1301 Wireless Power Transmission for Sustainable Electronics (WiPE). He is Associate Editor of IEEE Wireless Communication Letters since its foundation and Technical Program Committee (TPC) member of flagship IEEE conferences. He holds two patents from USPTO and he was recently included in https://sites.google.com/site/highlycited/highly-cited-greek-scientists.

Dr. Bletsas was the co-recipient of IEEE Communications Society 2008 Marconi Prize Paper Award in Wireless Communications, best paper distinction in ISWCS 2009, Siena, Italy, Second Best Student Paper Award in the IEEE RFID-TA 2011, Sitges, Barcelona, Spain, best paper distinction in IEEE Sensors Conference (SENSORS), November 2013, Baltimore, USA and best student paper award in IEEE ICASSP 2015, Brisbane, Australia. Two of his undergraduate advisees were winners of the 2009-2011 and 2011-2012, respectively, best Diploma Thesis contest among all Greek Universities on "Advanced Wireless Systems," awarded by IEEE VTS/AES joint Greek Chapter. At the end of 2013, Dr. Bletsas was awarded the Technical University of Crete 2013 Research Excellence Award.